Cooperative Time and Energy-Optimal Lane Change Maneuvers for Connected Automated Vehicles

Rui Chen, Christos G. Cassandras, *Life Fellow, IEEE*, Amin Tahmasbi-Sarvestani, Shigenobu Saigusa, Hossein Nourkhiz Mahjoub, *Member, IEEE*, and Yasir Khudhair Al-Nadawi

***Abstract*— We derive optimal control policies for a Connected Automated Vehicle (CAV) cooperating with neighboring CAVs in order to implement a lane change maneuver consisting of a longitudinal phase where the CAV properly positions itself relative to the cooperating neighbors and a lateral phase where it safely changes lanes. For the first phase, we optimize the maneuver time subject to safety constraints and subsequently minimize the associated surrogate energy consumption of all cooperating vehicles in this maneuver. For the second phase, we jointly optimize time and energy approximation and provide three different solution methods including a real-time approach based on Control Barrier Functions (CBFs). We prove structural properties of the optimal policies which simplify the solution derivations and, in the case of the longitudinal maneuver, lead to analytical optimal control expressions. The solutions, when they exist, are guaranteed to satisfy safety constraints for all vehicles involved in the maneuver. Simulation results where the controllers are implemented show their effectiveness in terms of significant performance improvements compared to maneuvers performed by human-driven vehicles.**

***Index Terms*— Autonomous vehicles, intelligent vehicles, cooperative systems, optimal control.**

I. Introduction

ADVANCES in transportation system technologies and the emergence of Connected and Automated Vehicles (CAVs), also known as "autonomous vehicles", have the potential to drastically improve a transportation network's performance in terms of safety, comfort, congestion reduction and energy efficiency. The motivation for minimizing energy in transportation systems is well-documented in the literature and comes from the need to lower fuel costs and pollution levels for the sake of improving public health and the environment [1], [2]. In highway driving, an overview of automated intelligent vehicle-highway systems was provided in [3] with more recent developments mostly focusing on autonomous car-following control [4]–[6]. In urban driving, efforts have concentrated on controlling traffic lights [7] or the cooperative control of CAVs through non-signalized intersections [8], [9].

Automating a lane change maneuver remains a challenging problem which has attracted increasing attention in recent years [10]–[13]. Designing such an automated maneuver is often viewed as consisting of two levels [14]: at the strategy level, a feasible (possibly optimal in some sense) trajectory is generated for lane changing; then, the control level is responsible for determining how vehicles track the aforementioned trajectory. For example, [12] adopts such a design architecture for an automated lane-change maneuver, but does not provide an analytical solution and assumes that there are no other vehicles in the left lane (the lane in which the controllable vehicle ends up after completing the maneuver). In [15], background vehicles are included in the left lane and the goal is to check whether there exists a feasible lane-change trajectory or not; if one exists, the controllable vehicle will then track this trajectory. A similar approach is taken in [16] with the trajectory being updated during the maneuver based on the latest surrounding information. In these papers, only one vehicle can be controlled during the maneuver and no analytical solutions are provided.

The emergence of CAVs creates the opportunity for cooperation among vehicles traveling in both left and right lanes in carrying out an automated lane-change maneuver [14], [17], [18], [19]–[21]. Such cooperation presents several advantages relative to the two-level architecture mentioned above. In particular, when controlling a single vehicle and checking on the feasibility of a maneuver depending on the state of nearby traffic, as in [22], [23], the maneuver is often infeasible without the cooperation of other vehicles, especially under heavier traffic conditions. In contrast, a cooperative approach can allow multiple interacting vehicles to implement controllers enabling a larger set of maneuvers. Aside from enhancing safety, this cooperative behavior can also improve the throughput, hence reducing the chance of congestion. Feasible, but not necessarily optimal, vehicle trajectories for cooperative multi-agent lane-changing maneuvers are derived in [1]. The case of multiple cooperating vehicles simultaneously changing lanes is considered in [2] with the requirement that all vehicles

Manuscript received January 14, 2020; revised May 26, 2020, August 23, 2020, and October 19, 2020; accepted October 30, 2020. This work was supported in part by the Honda Research and Development Americas, Inc.; in part by NSF under Grant ECCS-1931600, Grant DMS-166464, and Grant CNS-1645681; in part by the Air Force Office of Scientific Research (AFOSR) under Grant FA9550-19-1-0158; in part by the Advanced Research Project Agency-Energy's (ARPA-E's) NEXTCAR Program under Grant DE-AR0000796; and in part by the MathWorks. The Associate Editor for this article was H. Jula. *(Corresponding author: Rui Chen.)*

Rui Chen and Christos G. Cassandras are with the Division of Systems Engineering, Boston University, Boston, MA 02446 USA, and also with the Center for Information and Systems Engineering, Boston University, Boston, MA 02446 USA (e-mail: ruic@bu.edu; cgc@bu.edu).

Amin Tahmasbi-Sarvestani was with Honda Research and Development Americas, Inc., Ann Arbor, MI 48103 USA. He is now with Optimus Ride, Inc., Boston, MA 02210 USA (e-mail: atahmasbig@hra.com).

Shigenobu Saigusa, Hossein Nourkhiz Mahjoub, and Yasir Khudhair Al-Nadawi are with Honda Research and Development Americas, Inc., Ann Arbor, MI 48103 USA (e-mail: ssaigusa@hra.com; hnourkhizmahjoub@hra.com; yalnadawi@hra.com).

Digital Object Identifier 10.1109/TITS.2020.3036420

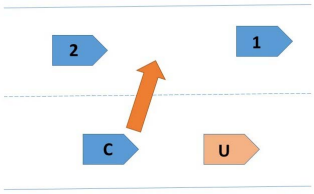

Fig. 1. The basic lane changing maneuver process.

are controllable and their velocities prior to the lane change are all the same. First, vehicles with a lower priority must adjust their positions in their current lane and give way to those with a higher priority so as to avoid collisions. Then, a lane changing optimal control problem is solved for each vehicle without considering the usual safe distance constraints between vehicles. This "progressively constrained dynamic optimization" method facilitates a numerical solution to the underlying optimal control problem at the expense of some loss in performance.

Our goal in this paper is to provide an optimal solution for the maneuver in Fig. 1, in which the controlled vehicle C attempts to overtake an uncontrollable vehicle U by using the left lane to pass. In this case, the initial velocities of all vehicles can be different and arbitrary. The overall lane changing and passing maneuver consists of three steps: (i) The target vehicle C moves to the left lane, (ii) C moves faster than U (and possibly other vehicles ahead of it) while on the left lane, (iii) C performs a second lane-changing maneuver so as to move back to the right lane. We will limit ourselves to the first step which, in turn, consists of two parts. First, vehicle C adjusts its position in the current lane to prepare for a lane shift, while vehicles 1 and 2 in Fig. 1 cooperate to create space for C in the left lane. Next, the lateral lane shift of C takes place. Our objective is to minimize both the maneuver time and the energy consumption of vehicles C, 1 and 2 which are all assumed to share their state information. We also impose a hard safe distance constraint between all adjacent vehicles located in the same lane, as well as constraints due to speed and acceleration limits imposed on all vehicles. In the longitudinal phase of the maneuver (introduced in [24]), we first determine a minimum feasible time subject to all constraints for vehicles C, 1 and 2. We then solve a fixed terminal time decentralized optimal control problem for each of the three vehicles seeking to minimize the energy consumed. In the lateral phase, we solve a decentralized optimal control problem seeking to jointly minimize the time and energy consumed. In both cases, we derive several properties of the optimal control which facilitate obtaining explicit solutions, hence leading to real-time implementability. Our approach applies to a wider range of scenarios relative to those in [15], [16], [22], [23] and incorporates the safety distance constraint not included in [1] and [2]. Compared with [24], this paper contains all proofs of the main results, the lateral component of the lane change maneuvers studied, and several new simulation results, including the lateral part of the maneuvers.

The rest of this paper is organized as follows. Section II formulates the lane-change maneuver problem along the longitudinal direction. In Section III, a complete optimal control solution for the longitudinal phase is obtained. Section IV addresses the lateral maneuver followed with the combination of both maneuvers in Section V. Section VI provides simulation results for several representative examples and we conclude with Section VII.

II. Problem Formulation for the Longitudinal Maneuver

We define $x_i(t)$ to be the longitudinal position of vehicle i along its current lane measured with respect to a given origin, where we use $i = 1, 2, C, U$. Similarly, $v_i(t)$ and $u_i(t)$ are vehicle i's velocity and (controllable) acceleration. The dynamics of vehicle i are

$$\dot{x}_i(t) = v_i(t), \quad \dot{v}_i(t) = u_i(t) \tag{1}$$

The maneuvers carried out by vehicles $1, 2, C$ are initiated at time t_0 and end at time t_f. We define $d_i(v_i(t))$ to be the minimal safe distance between vehicle i and the one that precedes it in its lane; this, in general, depends on the vehicle's current speed. The control input and speed are constrained as follows for all $t \in [t_0, t_f]$:

$$u_{i\min} \le u_i(t) \le u_{i\max}, \quad v_{i\min} \le v_i(t) \le v_{i\max} \tag{2}$$

where $u_{i\max}$, $u_{i\min}$, $v_{i\max}$, $v_{i\min}$ are the maximal and minimal acceleration (respectively speed) limits. In Fig. 1, we control vehicles 1, 2 and C to complete a lane change maneuver while minimizing the maneuver time and the corresponding surrogate energy consumption. For each vehicle $i = 1, 2, C$ we formulate the following optimization problem assuming that $x_i(0)$ and $v_i(0)$ are given:

$$\begin{aligned} &J(t_f; u_i(t)) \\ &= \min_{u_i(t)} \int_0^{t_f} [w_t + [w_{1,u}u_1^2(t) + w_{2,u}u_2^2(t) + w_{C,u}u_C^2(t)]]dt \\ &\quad \text{s.t. (1), (2) and} \\ &\qquad x_1(t) - x_2(t) \ge d_2(v_2(t)), \quad t \in [0, t_f] \\ &\qquad x_U(t) - x_C(t) \ge d_C(v_C(t)), \quad t \in [0, t_f] \\ &\qquad x_1(t_f) - x_C(t_f) \ge d_C(v_C(t_f)), \\ &\qquad x_C(t_f) - x_2(t_f) \ge d_2(v_2(t_f)) \end{aligned} \tag{3}$$

where w_t, w_u are weights associated with the maneuver time t_f and with a measure of the total surrogate energy expended. The two terms in (3) need to be properly normalized, therefore, we set $w_t = \frac{\rho}{T_{\max}}$ and $w_{i,u} = \frac{1-\rho}{\max\{u_{i\max}^2, u_{i\min}^2\}}$, where $\rho \in [0, 1]$ and $T_{\max}$ is a prespecified upper bound on the maneuver time (e.g., $T_{\max} = l/\min\{v_{i\min}\}$, $i = 1, 2, C, U$, where l is the distance to the next highway exit). Clearly, if $\rho = 0$ this problem reduces to an energy minimization problem and if $\rho = 1$ it reduces to minimizing the maneuver time. The safe distance is defined as $d_i(v_i(t)) = \phi v_i(t) + \delta$ where ϕ is the headway time (the general rule $\phi = 1.8$ is usually adopted as in [25]). It is shown in [26] that $u_i^2(t)$ may be used as an approximation of energy (a surrogate function) as it captures the monotonic dependence on acceleration while allowing us to derive an analytical solution. This approach is

also supported in [27] by experiments based on very detailed energy models showing results consistent with this simple model. Another way of justifying the $u_i^2(t)$ metric is that its minimization results in the smoothest possible lane-changing maneuver. As stated, the problem allows for a free terminal time t_f and terminal state constraints $x_i(t_f)$, $v_i(t_f)$. In the next section, we will specify the terminal time t_f as the solution of a minimization problem which allows each vehicle to specify a desired "aggressiveness level" relative to the shortest possible maneuver time subject to (2). Based on that, we will also specify $x_i(t_f)$, $i = 1, 2, C$. Finally, with the derived terminal time and position, we will derive the optimal control solution for every controllable CAV.

III. Optimal Control Solution for the Longitudinal Maneuver

Terminal Time Specification: We begin by formulating the following minimization problem based on which the maneuver terminal time t_f is specified:

$$\min_{t_f>0} \; t_f \tag{4}$$

$$\text{s.t. } x_1(0) + v_1(0)t_f + 0.5\alpha_1 u_{1\max} t_f^2 - x_C(0) - v_C(0)t_f - 0.5\alpha_C u_{C\max} t_f^2 \geq d_C(v_C(t_f)) \tag{4a}$$

$$x_U(t_f) - x_C(0) - v_C(0)t_f - 0.5\alpha_C u_{C\min} t_f^2 \geq d_C(v_C(t_f)) \tag{4b}$$

$$x_C(0) + v_C(0)t_f + 0.5\alpha_C u_{C\min} t_f^2 - x_2(0) - v_2(0)t_f - 0.5\alpha_2 u_{2\min} t_f^2 \geq d_2(v_2(t_f)) \tag{4c}$$

where $\alpha_i \in [0, 1), i = 1, 2, C$ is an "aggressiveness coefficient" for vehicle i which can be preset by the driver. Observe that $[x_i(t_0) + v_i(t_0)t_f + 0.5\alpha_i u_{i\max} t_f^2]$ is the terminal position of i under control $\alpha_i u_{i\max}$. To minimize t_f, vehicle 1 should accelerate and vehicle 2 decelerate so as to increase the gap between them in Fig. 1. If C accelerates, then (4a) ensures the safety constraint is still satisfied. If C has to decelerate because it is constrained by U, then (4b) ensures that the safety constraint between U and C is satisfied and (4c) ensures that the safety constraint between 2 and C is also satisfied. As we will subsequently show, the optimal control of C is either always non-positive or always non-negative throughout $[0, t_f]$ so that either the first or the last two constraints are relevant to it. Naturally, a solution to (4) may not exist, in which case we must iterate on the values of α_i until one is possibly identified. If that is not possible, then the maneuver is clearly aborted. If a solution t_f to (4) exists, we will specify a terminal position $x_i(t_f)$ next and check the feasibility of $(x_i(t_f), t_f)$ later in this section.

Terminal Position Specifications: Assuming a solution t_f is determined through (4), we next seek to specify terminal vehicle positions $x_i(t_f)$, $i = 1, 2, C$, to be associated with problem (3). To do so, we define

$$\Delta x_i(t_f) = x_i(t_f) - x_i(t_0) - v_i(t_0)t_f$$

which is the difference between the actual terminal position of i and its "ideal" terminal position under constant speed $v_i(t_0)$; this is ideal from the energy point of view in (5), since (once t_f is specified) the approximation of energy component is minimized when $u_i(t) = 0$. Thus, the energy-optimal value is $\Delta x_i(t_f) = 0$. We then seek terminal positions that minimize a measure of deviating form these energy-optimal values over all three vehicles:

$$\begin{aligned} \min_{x_i(t_f)>x_i(0), i=1,2,C} \; & \Delta x_C^2(t_f) + \Delta x_1^2(t_f) + \Delta x_2^2(t_f) \\ \text{s.t. } & \Delta x_i(t_f) = x_i(t_f) - x_i(0) - v_i(t_0)t_f \\ & x_1(t_f) - x_C(t_f) \geq \max\{d_C(v_C(t))\} \\ & x_C(t_f) - x_2(t_f) \geq \max\{d_2(v_2(t))\} \\ & x_U(t_f) - x_C(t_f) \geq \max\{d_C(v_C(t))\} \end{aligned} \tag{5}$$

The $\max\{\cdot\}$ values in (5) are assumed to be given by a prespecified maximum inter-vehicle safe distance. However, as subsequently shown in Theorem 1, they actually turn out to be the known initial or terminal values of $d_2(v_2(t))$ and $d_C(v_C(t))$. For example, $\max\{d_2(v_2(t))\} = d_2(v_2(t_0))$ and $\max\{d_C(v_C(t))\} = d_C(v_C(t_0) + u_{C\max} t_f)$.

Lemma 1: The solution $x_i^*(t_f)$, $i = 1, 2, C$, to (5) satisfies $\Delta x_1^*(t_f) \geq 0$ and $\Delta x_2^*(t_f) \leq 0$.

Proof: See Appendix. ■

In the next two subsections, we formulate and solve the optimal control problems for vehicles 1, 2 and then C.

A. Optimal Control of Vehicles 1 and 2

With the terminal time t_f and longitudinal position $x_i(t_f)$, $i = 1, 2$, set through (4) and (5) respectively, the optimal control problems of vehicles $i = 1, 2$ in (3) become:

$$\min_{u_1(t)} \int_0^{t_f} \frac{1}{2} u_1^2(t)dt \quad \text{s.t. (1), (2), } x_1(t_f) = x_{1,f} \tag{6}$$

$$\min_{u_2(t)} \int_0^{t_f} \frac{1}{2} u_2^2(t)dt \quad \text{s.t. (1), (2), } x_2(t_f) \leq x_{2,f}, \; x_1(t) - x_2(t) \geq d_2(v_2(t)), \quad t \in [0, t_f] \tag{7}$$

where $x_{1,f}$ and $x_{2,f}$ are given above. In (7), we use an inequality $x_2(t_f) \leq x_{2,f}$ to describe the terminal position constraint instead of the equality since it suffices for the distance between the two vehicles to accommodate vehicle C while at the same time allowing for the cost under a control with $x_2(t_f) < x_{2,f}$ to be smaller than under a control with $x_2(t_f) = x_{2,f}$. In (6), there is no need to consider the case that $x_1(t_f) > x_{1,f}$ since it is clear that the optimal cost when $x_1(t_f) = x_{1,f}$ is always smaller compared to $x_1(t_f) > x_{1,f}$.

The next result establishes the fact that the solution of these two problems involves vehicle 1 never decelerating and vehicle 2 never accelerating.

Theorem 1: The optimal control in (6) is $u_1^*(t) \geq 0$ and the optimal control in (7) is $u_2^*(t) \leq 0$.

Proof :See Appendix. ■

Based on Theorem 1, in addition to showing that vehicle 1 never decelerates and vehicle 2 never accelerates, we also eliminate the safe distance constraint in (7) since the distance between the vehicles will increase in the course of the maneuver and the last two safety constraints in (3) ensure that this distance is eventually large enough to accommodate the length

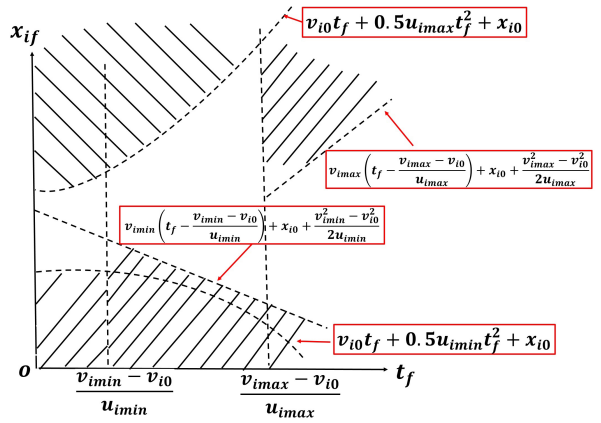

Fig. 2. The feasible state set of controllable vehicles in the left lane.

of vehicle C. Thus, (7) becomes

$$\min_{u_2(t)} \int_0^{t_f} \frac{1}{2}u_2^2(t)dt \quad \text{s.t.} \quad (1), (2), x_2(t_f) = x_{2,f} \tag{8}$$

1) Feasible Terminal State Set: The constraints in (2) limit the sets of feasible terminal conditions $(x_{i,f}, t_f)$, $i = 1, 2, C$ as shown in Fig. 2 where the feasible set is the unshaded area defined as follows for each $i = 1, 2, C$:

(i) Vehicle i cannot reach $x_{i,f}$ under its maximal acceleration if $u_{i\max}t_f + v_{i,0} \le v_{i\max}$ and $v_{i,0}t_f + 0.5u_{i\max}t_f^2 < x_{i,f} - x_{i,0}$.

(ii) Vehicle i cannot reach $x_{i,f}$ under its maximal acceleration after attaining its maximal velocity if $u_{i\max}t_f + v_{i,0} > v_{i\max}$ and $v_{i\max}(t_f - \frac{v_{i\max}-v_{i,0}}{u_{i\max}}) < x_{i,f} - x_{i,0} - \frac{v_{i\max}^2 - v_{i,0}^2}{2u_{i\max}}$.

(iii) Vehicle i exceeds $x_{i,f}$ under the minimal acceleration if $u_{i\min}t_f + v_{i,0} \ge v_{i\min}$ and $v_{i,0}t_f + 0.5u_{i\min}t_f^2 > x_{i,f} - x_{i,0}$.

(iv) Vehicle i exceeds $x_{i,f}$ under the minimal acceleration after attaining its minimal velocity if $u_{i\min}t_f + v_{i,0} < v_{i\min}$ and $v_{i\min}(t_f - \frac{v_{i\min}-v_{i,0}}{u_{i\min}}) > x_{i,f} - x_{i,0} - \frac{v_{i\min}^2 - v_{i,0}^2}{2u_{i\min}}$.

In addition, vehicle C must also satisfy a safety distance constraint with respect to vehicle U, hence if $x_{C,f} > x_U(0) + v_U t_f - d_C(v_2(t_f))$, there is no feasible solution.

Note that if an optimal t_f is determined in (4) and the solution of (5) guarantees that $x_i(t_f)$, $i = 1, 2, C$, do not violate the safety constraints, $(x_{i,f}, t_f)$ is expected to be feasible. However, if $(x_{i,f}, t_f)$ is infeasible for vehicle i, then the following Algorithm 1 is used to find a feasible such pair:

Algorithm 1 Determine the Feasible Pair $(x_{i,f}, t_f)$

```
Judge=1;
while Judge=1 do
    t_f = βt_f, β > 1 ;
    Solve (5) to obtain new x_{i,f} with updated t_f;
    if (x_{i,f}, t_f) is feasible then
        Judge=0;
    end
end
```

In the above, the adjustable coefficient β is used to relax the maneuver time t_f so as to accommodate one or more of the constraints in Fig. 2 until a feasible $(x_{i,f}, t_f)$ is identified.

2) Solution of Problem (6): We can now proceed to derive an explicit solution for (6) taking advantage of Theorem 1. We begin by writing the Hamiltonian and associated Lagrangian functions for (6):

$$H(v_1, u_1, \lambda) = \frac{1}{2}u_1^2(t) + \lambda_x(t)v_1(t) + \lambda_v(t)u_1(t) \tag{9}$$

$$\begin{aligned} L(v_1, u_1, \lambda, \eta) = {} & H(v, u, \lambda) + \eta_1(t)(u_{1\min} - u_1(t)) \\ & + \eta_2(t)(u_1(t) - u_{1\max}) \\ & + \eta_3(t)(v_{1\min} - v_1(t)) \\ & + \eta_4(t)(v_1(t) - v_{1\max}) \end{aligned} \tag{10}$$

where $\lambda(t) = [\lambda_v(t), \lambda_x(t)]^T$ is the costate vector and $\eta = [\eta_1(t), ..., \eta_4(t)]^T$. In view of Theorem 1, i.e., $u_1^*(t) \ge 0$, (10) reduces to

$$\begin{aligned} L(v_1, u_1, \lambda, \eta) = {} & \frac{1}{2}u_1^2(t) + \lambda_x(t)v_1(t) + \lambda_v(t)u_1(t) \\ & + \eta_2(t)(u_1(t) - u_{1\max}) + \eta_3(t)(v_{1\min} - v_1(t)) \\ & + \eta_4(t)(v_1(t) - v_{1\max}) \end{aligned} \tag{11}$$

The explicit solution of (6) is given next.

Theorem 2: Let $x_1^*(t)$, $v_1^*(t)$, $u_1^*(t)$ be a solution of (6). Then,

$$u_1^*(t) = \arg \min_{0 \le u_1 \le u_{1\max}} \frac{1}{2}[u_1^2 + \frac{u_1^*(t_0)^2(t-\tau)u_1}{v_{1,0} - v_1^*(t_f) + (\tau - t_0)u_1^*(t_0)}] \tag{12}$$

where $\tau \in [t_0, t_f)$ is the first time that $v_1^*(\tau) = v_{1\max}$ and $\tau = t_f$ if $v_{1\max}$ is never reached.

Proof: See Appendix. ■

The expression in (12) provides sufficient information to allow the explicit evaluation of $u_1^*(t)$ over all $t \in [t_0, t_f]$. In particular, either $u_1^*(t) = u_{1max}$ or it is the solution of the simple quadratic minimization problem in (12). Furthermore, following a derivation similar to that in [28] we can obtain the optimal cost $J_1^*(t_f)$ in (6) based on several cases depending on the initial acceleration $u_{1,0}^* \equiv u_1^*(t_0)$ and the terminal velocity $v_1^*(t_f)$ which can be explicitly evaluated as in [28]. The final optimal cost is the minimal among all possible values obtained.

Case I: $u_{1,0}^* = u_{1\max}$ and $\dot{u}_1^*(t) = 0$. If $t_f < \frac{v_{1\max}-v_{1,0}}{u_{1\max}}$, then $u_1^*(t) = u_{1\max}$ for all $t \in [0, t_f]$. Otherwise, when $v_1(t) = v_{1\max}$, the control switches to $u_1^*(t) = 0$. Therefore,

$$J_1^*(t_f) = \begin{cases} \frac{1}{2}u_{1\max}(v_{1\max} - v_{1,0}) & \text{if } t_f \ge \frac{v_{1\max} - v_{1,0}}{u_{1\max}} \\ \frac{1}{2}u_{1\max}^2(t_f - t_0) & \text{otherwise} \end{cases} \tag{13}$$

Case II: $u_{1,0}^* = u_{1\max}$ and $v_1^*(t_f) = v_{1\max}$. We define t_1 as the time that $u_1^*(t)$ begins to decrease and τ as the first time that $u_1^*(\tau) = 0$. Thus, $u_1^*(t)$ is a piecewise linear function of time t and (following calculations similar to those in [28]):

$$J_1^*(t_f) = \frac{1}{2}(t_1 - t_0)u_{1\max}^2 + \frac{1}{24}\frac{u_{1\max}^4(\tau - t_1)^3}{[v_{1,0} - v_{1\max} + (\tau - t_0)u_{1\max}]^2} \tag{14}$$

Using similar calculations, we summarize below the remaining three cases:

$$\textbf{Case III}: \begin{matrix} u_{1,0}^* = u_{1\max} \\ v_1^*(t_f) < v_{1\max} \end{matrix} \quad J_1^*(t_f) = \frac{1}{2}\frac{u_{1\max}^2(t_f+2t_1-3t_0)}{3}$$

$$\textbf{Case IV}: \begin{matrix} u_{1,0}^* < u_{1\max} \\ v_1^*(t_f) = v_{1\max} \end{matrix} \quad J_1^*(t_f) = \frac{2}{3}\frac{(v_{1\max}-v_{1,0})^2}{\tau - t_0}$$

$$\textbf{Case V}: \begin{matrix} u_{1,0}^* < u_{1\max} \\ v_1^*(t_f) < v_{1\max} \end{matrix} \quad J_1^*(t_f) = \frac{3}{2}\frac{[x_{1,f}-v_{1,0}(t_f-t_0)]^2}{(t_f-t_0)^3}$$

3) Solution of Problem (7): Similar to the solution of (6), we can derive an explicit solution for (8) taking advantage of Theorem 1 and obtain the following result.

Theorem 3: Let $x_2^*(t)$, $v_2^*(t)$, $u_2^*(t)$ be a solution of (8). Then,

$$u_2^*(t) = \arg\min_{u_{2\min}\le u_2\le 0} \frac{1}{2}[u_2^2 + \frac{u_2^*(t_0)^2(\tau-t)u_2}{v_2^*(t_f)-v_{2,0}-(\tau-t_0)u_2^*(t_0)}] \tag{15}$$

where $\tau \in [t_0, t_f)$ is the first time that $v_2^*(\tau) = v_{2\min}$ and $\tau = t_f$ if $v_{2\min}$ is never reached.

Proof: See Appendix. ■

We can also obtain the optimal cost $J_2^*(t_f)$ in (7) based on several cases depending on the initial acceleration $u_{2,0}^*$ and the terminal velocity $v_2^*(t_f)$ which can be explicitly evaluated as in [28]. In what follows, we define t_1 as the time that $u_2^*(t)$ begins to increase and τ as the first time that $u_2^*(\tau) = 0$.

$$\textbf{Case I}: \begin{matrix} u_{2,0}^* = u_{2\min} \\ v_2^*(t_f) = v_{2\min} \end{matrix} \quad \begin{matrix} J_2^*(t_f) = \frac{1}{2}(t_1-t_0)u_{2\min}^2 \\ +\frac{1}{24}\frac{u_{2\min}^4(\tau-t_1)^3}{[v_{2,0}-v_{2\min}+(\tau-t_0)u_{2\min}]^2} \end{matrix}$$

$$\textbf{Case II}: \begin{matrix} u_{2,0}^* = u_{2\min} \\ v_2^*(t_f) > v_{2\min} \end{matrix} \quad J_2^*(t_f) = \frac{u_{2\min}^2(t_f+2t_1-3t_0)}{6}$$

$$\textbf{Case III}: \begin{matrix} u_{2,0}^* > u_{2\min} \\ v_2^*(t_f) = v_{2\min} \end{matrix} \quad J_2^*(t_f) = \frac{2}{3}\frac{(v_{2\min}-v_{2,0})^2}{\tau - t_0}$$

$$\textbf{Case IV}: \begin{matrix} u_{2,0}^* > u_{2\min} \\ v_2^*(t_f) = v_{2\min} \end{matrix} \quad J_2^*(t_f) = \frac{3}{2}\frac{[x_{2,f}-v_{2,0}(t_f-t_0)]^2}{(t_f-t_0)^3}$$

B. Optimal Control of Vehicle C

Unlike (6) and (8), deriving the optimal control of vehicle C as in Fig. 1 is more challenging. First, since we need to keep a safe distance between vehicles C and U, a constraint $x_U(0) + v_U t - x_C(t) \ge d_C(v_C(t))$ must hold for all $t \in [0, t_f]$. The resulting problem formulation is:

$$\begin{aligned} &\min_{u_C(t)} \int_0^{t_f} \frac{1}{2}u_C^2(t)dt \\ &\text{s.t. (1), (2)}, \quad x_C(t_f) = x_{C,f}, \ t \in [0, t_f] \\ &\qquad x_U(0) + v_U t - x_C(t) \ge d_C(v_C(t)) \end{aligned} \tag{16}$$

in which $d_C(v_C(t))$ is time-varying. To simplify (16), we use d_C as a constant value instead of $d_C(v_C(t))$. Especially, users can set $d_C \equiv max\{d_C\}$ to derive a more conservative constraint still ensuring that the original one is not violated (the problem with $d_C(v_C(t)) = \phi v_C(t) + \delta$ can still be solved at the expense of added complexity and is the subject of ongoing research).

The Hamiltonian for (16) with the constraints adjoined yields the Lagrangian

$$\begin{aligned} &L(x_C, v_C, u_C, \lambda, \eta) \\ &\quad = \frac{1}{2}u_C^2(t) + \lambda_x(t)v_C(t) + \lambda_v(t)u_C(t) \\ &\qquad + \eta_1(t)(u_C(t) - u_{C\max}) + \eta_2(t)(u_{C\min} - u_C(t)) \\ &\qquad + \eta_3(t)(v_C(t) - v_{C\max}) + \eta_4(t)(v_{C\min} - v_C(t)) \\ &\qquad + \eta_5(t)(x_C(t) - x_U(0) - v_U(0)t + d_C) \end{aligned} \tag{17}$$

with $\lambda(t) = [\lambda_v(t), \lambda_x(t)]^T$ and $\eta = [\eta_1(t), ..., \eta_5(t)]^T$, $t \in [0, t_f]$. Based on Pontryagin's principle, we have

$$u_C^*(t) = \begin{cases} -\lambda_v(t) & \text{if } u_{C\min} \le -\lambda_v(t) \le u_{C\max} \\ u_{C\min} & \text{if } -\lambda_v(t) < u_{C\min} \\ u_{C\max} & \text{if } -\lambda_v(t) > u_{C\max} \end{cases} \tag{18}$$

when none of the constraints is active along an optimal trajectory. In order to account for the constraints becoming active, we identify several cases depending on the terminal states of vehicles U and C. Let us define $\bar{x}_C(t_f)$ to be the terminal position of C if $u_C(t) = 0$ for all $t \in [0, t_f]$. The relationship between $\bar{x}_C(t_f)$ and $x_C(t_f)$ is critical. In particular, if $\bar{x}_C(t_f) < x_C(t_f)$, vehicle C must accelerate in order satisfy the terminal position constraint. Otherwise, C must decelerate. Also critical is the value of $x_U(t_f) - d_C$, i.e., the upper bound of the safe terminal position of C. In addition, during the entire maneuver process, we require that $x_C(t) \le x_U(t) - d_C$.

We begin with the 3! cases for ordering $x_C(t_f)$, $\bar{x}_C(t_f)$ and $x_U(t_f) - d_C$ as follows: $\bar{x}_C(t_f) \le x_C(t_f) \le x_U(t_f) - d_C$; $\bar{x}_C(t_f) \le x_U(t_f) - d_C \le x_C(t_f)$; $x_C(t_f) \le \bar{x}_C(t_f) \le x_U(t_f) - d_C$; $x_C(t_f) \le x_U(t_f) - d_C \le \bar{x}_C(t_f)$; $x_U(t_f) - d_C \le \bar{x}_C(t_f) \le x_C(t_f)$; $x_U(t_f) - d_C \le x_C(t_f) \le \bar{x}_C(t_f)$. Fortunately, we can exclude several cases as infeasible because $x_C(t_f) \le x_U(t_f) - d_C$ is a necessary condition to have feasible solutions. This leaves three remaining cases as follows. *Case 1*: $\bar{x}_C(t_f) \le x_C(t_f) \le x_U(t_f) - d_C$. *Case 2*: $x_C(t_f) \le \bar{x}_C(t_f) \le x_U(t_f) - d_C$. *Case 3*: $x_C(t_f) \le x_U(t_f) - d_C \le \bar{x}_C(t_f)$.

These are visualized in Fig. 3. The following results provide structural properties of the optimal solution (18) depending on which case applies.

Lemma 2: If $x_U(0) + v_U(0)t - x_C(t) = d_C$, then $v_C(t) = v_U(0)$, $t \in [0, t_f]$.

Proof: See Appendix. ■

Theorem 4 (Case 1 in Fig. 3): If $\bar{x}_C(t_f) \le x_C(t_f) \le x_U(t_f) - d_C$, then $u_C^*(t) \ge 0$ and $\eta_5^*(t) = 0$ for all $t \in [0, t_f)$.

Proof: See Appendix. ■

Theorem 5 (Case 2 in Fig. 3): If $x_C(t_f) \le \bar{x}_C(t_f) \le x_U(t_f) - d_C$, then $u_C^*(t) \le 0$ and $\eta_5^*(t) = 0$ for all $t \in [0, t_f)$.

Proof: The proof is similar to that of Theorem 4 and is omitted. ■

Theorem 6 (Case 3 in Fig. 3): If $x_C(t_f) \le x_U(t_f) - d_C \le \bar{x}_C(t_f)$, then $u_C^*(t) \le 0$.

Proof: See Appendix. ■

Based on Theorems 4,5, *Cases 1,2* in Fig. 3 can be solved without the safety constraint in (16) since we have shown that $\eta_5^*(t) = 0$. Therefore, the optimal control is the same as that derived for vehicles 1 and 2 in Theorems 2,3. This leaves only *Case 3* to analyze. We proceed by first solving (16)

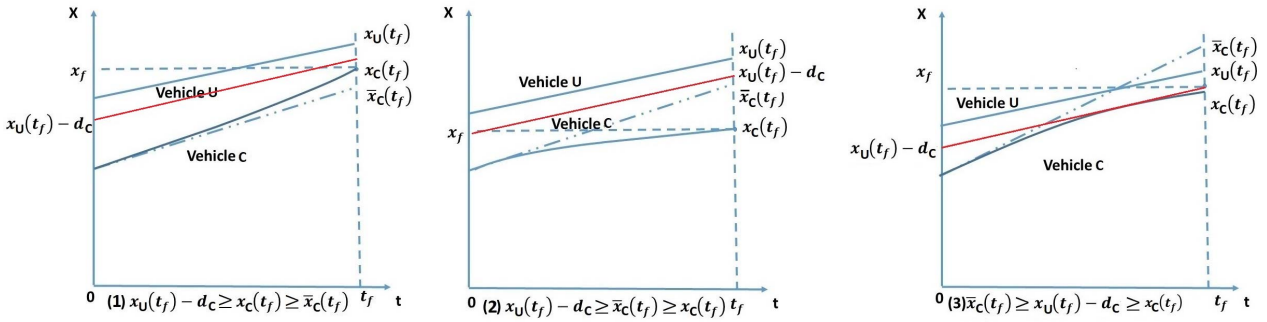

Fig. 3. The three feasible cases for the optimal maneuver of vehicle C.

without the safety constraint, so it reduces to the solution in Theorem 3, since we know that $u_C^*(t) \leq 0$. If a feasible optimal solution exists, then the problem is solved. Otherwise, we need to re-solve the problem in order to determine an optimal trajectory that includes at least one arc in which $x_U(0) + v_U(0)t - x_C^*(t) - d_C = 0$.

Based on Lemma 2, there exists a time $\tau_1 \in (0, t_f)$ that satisfies $v_C(\tau_1) = v_U(0)$ and $x_C(\tau_1) = x_U(0) + v_U(0)\tau_1 - d_C \equiv a$ (it is easy to see that there is at most one such constrained arc, since $v_C(t) = v_U(0)$ as soon as this arc is entered.) We then split problem (16) into two subproblems as follows:

$$\begin{aligned} &\min_{u_C(t)} \int_0^{\tau_1} \frac{1}{2} u_C^2(t) dt \\ &\text{s.t. (1), (2)}, \quad x_C(\tau_1) = a, \ v_C(\tau_1) = v_U(0), \ t \in [0, \tau_1) \end{aligned} \tag{19}$$

$$\begin{aligned} &\min_{u(t)} \int_{\tau_1}^{t_f} \frac{1}{2} u_C^2(t) dt \\ &\text{s.t. (1), (2)}, \quad x_C(\tau_1) = a, \quad v_C(\tau_1) = v_U(0), \\ &\qquad x_C(t_f) = x_{cf}, \ t \in [\tau_1, t_f] \end{aligned} \tag{20}$$

where (19) has a fixed terminal time τ_1 (to be determined), position a, and speed $v_U(0)$, while (20) has a fixed terminal time t_f and position $x_{C,f}$ with given $x_C(\tau_1) = a$.

Let us first solve (19). Since $u_C^*(t) \leq 0$ and the terminal speed is $v_U(0)$, only the acceleration constraint $u_{C\min} - u_C \leq 0$ can be active in $[0, \tau_1]$. Suppose that this constraint becomes active at time $\tau_2 < \tau_1$. Since $u_{C\min} - u_C$ is independent of t, $x_C(t)$, and $v_C(t)$, it follows (see [29]) that there are no discontinuities in the Hamiltonian or the costates, i.e., $\lambda_x(\tau_2^-) = \lambda_x(\tau_2^+)$, $\lambda_v(\tau_2^-) = \lambda_v(\tau_2^+)$, $H(\tau_2^-) = H(\tau_2^+)$. It follows from $H(\tau_2^-) - H(\tau_2^+) = 0$ and (17) that

$$[u_C^*(\tau_2^-) - u_C^*(\tau_2^+)][\frac{1}{2}(u_C^*(\tau_2^-)) + \frac{1}{2}(u_C^*(\tau_2^+)) + \lambda_v(\tau_2^-)] = 0$$

Therefore, either $u_C^*(\tau_2^-) = u_C^*(\tau_2^+)$ or $u_C^*(\tau_2^-) = -\lambda_v(\tau_2^-)$ based on (18). Either condition used in the above equation leads to the conclusion that $u_C^*(\tau_2^-) = u_C^*(\tau_2^+)$, i.e., $u_C^*(t)$ is continuous at τ_2.

Let us now evaluate the objective function in (19) as a function of τ_1 and a, denoting it by $J_1(\tau_1, a)$, under optimal control. In view of (18), there are two cases.

(a) $u_C^*(t) = u_{C\min}$ for $t \in [0, \tau_2)$, $u_C^*(t) = -\lambda_v(t)$ for $t \in [\tau_2, \tau_1]$. As in the proof of Theorem 2, the costate equations are $\dot{\lambda}_v(t) = -\lambda_x(t)$ and $\dot{\lambda}_x(t) = 0$. Therefore, $\lambda_v(t) = ct - b$ where b, c are to be determined. It follows that

$$u_C^*(t) = c(t - \tau_2) + u_{C\min}, \quad t \in [\tau_2, \tau_1) \tag{21}$$

and the following boundary conditions hold:

$$\begin{aligned} &v_C(\tau_2) = v_C(0) + u_{C\min}\tau_2 \\ &v_C(\tau_1) = v_U(0) = v_C(\tau_2) + \int_{\tau_2}^{\tau_1} [c(t - \tau_2) + u_{C\min}] dt \\ &x_C(\tau_2) = x_C(0) + v_C(0)\tau_2 + \frac{1}{2} u_{C\min}\tau_2^2 \\ &x_C(\tau_1) = a = x_C(\tau_2) + \int_{\tau_2}^{\tau_1} [\frac{c}{2}t^2 + (u_{C\min} - c\tau_2)(t - \tau_2) \\ &\qquad - \frac{c}{2}\tau_2^2 + v_C(0) + u_{C\min}\tau_2] dt \end{aligned} \tag{22}$$

Using (21) and (22) to eliminate c and τ_2 and then evaluate $J_1(\tau_1, a)$ in (19) after some algebra yields:

$$\begin{aligned} J_1(\tau_1, a) = &\frac{1}{2} u_{C\min}(2v_U(0) - 2v_C(0) - u_{C\min}\tau_1) \\ &+ \frac{2(v_U(0) - v_C(0) - u_{C\min}\tau_1)^3}{9(a - x_C(0) - v_C(0)\tau_1 - 0.5u_{C\min}\tau_1^2)} \end{aligned} \tag{23}$$

(b) $u_C^*(t) = -\lambda_v(t)$ for $t \in [0, \tau_2)$, $u_C^*(t) = u_{C\min}$ for $t \in [\tau_2, \tau_1]$. Proceeding as above, we derive

$$\begin{aligned} &v_C(\tau_2) = v_C(0) + \int_0^{\tau_2} [c(\tau_2 - t) + u_{C\min}] dt \\ &v_C(\tau_1) = v_U(0) = v_C(\tau_2) + (\tau_1 - \tau_2)u_{C\min} \\ &x_C(\tau_2) = x_C(0) + \int_0^{\tau_2} [v_C(0) + \frac{c}{2}t^2 + u_{C\min}t] dt \\ &x_C(\tau_1) = a = x_C(\tau_2) + \int_{\tau_2}^{\tau_1} [v_C(\tau_2) + u_{C\min}(t - \tau_2)] dt \end{aligned} \tag{24}$$

and, after some calculations, we obtain $J_1(\tau_1, a)$ in (19):

$$\begin{aligned} J_1(\tau_1, a) = &\frac{1}{2} u_{C\min}(2v_U(0) - 2v_C(0) - u_{C\min}\tau_1) \\ &- \frac{2(v_U(0) - v_C(0) - u_{C\min}\tau_1)^3}{9(a - x_C(0) - v_U\tau_1 + 0.5u_{C\min}\tau_1^2)} \end{aligned} \tag{25}$$

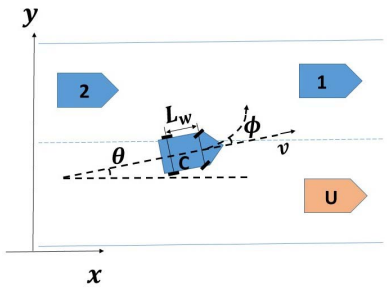

Fig. 4. Vehicle model over the lateral maneuver.

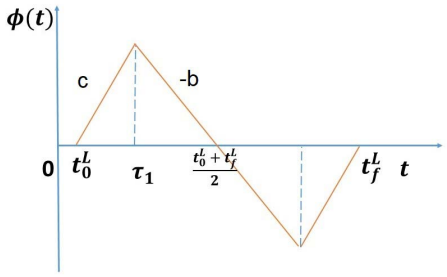

Fig. 5. The trajectory of ϕ(t) over the lateral maneuver.

Proceeding to the second subproblem (20), note that the control at the entry point of the constrained arc at time τ_1 is no longer guaranteed to be continuous. This problem is of the same form as the optimal control problem for vehicle 2 in (8) whose solution is given in Theorem 3, except that initial conditions now apply at time τ_1 as given in (20). Proceeding exactly as before, we can obtain the cost $J_2(\tau_1, a)$ under optimal control. Adding the two costs, we obtain $J_C(\tau_1, a) = J_1(\tau_1, a) + J_2(\tau_1, a)$ in (16). This results in a simple nonlinear programming problem whose solution (τ_1^*, a^*) results from setting $\frac{\partial J_C(\tau_1,a)}{\partial \tau_1} = 0$ and $\frac{\partial J_C(\tau_1,a)}{\partial a} = 0$. Finally, the optimal control is the one corresponding to (τ_1^*, a^*).

Based on our analysis, we find that *Case 3* is the only one where the safety constraint may become active. This provides an option to the vehicle C controller: if *Case 3* applies, the maneuver may either be implemented or it may be delayed until the conditions change to either one of *Cases 1,2* so as avoid the more complex situation that arises through (19),(20). As already stated, a lane change maneuver contains two components: a longitudinal part and a lateral part. We will next address the lateral maneuver component.

IV. Lateral Maneuver

Let t_0^L be the start time of the lateral phase of the lane-change maneuver. The most conservative approach is to set $t_0^L = t_f$, the optimal terminal time of the longitudinal phase as determined through (4). However, depending on the "aggressiveness" of a driver we may select $t_0^L \leq t_f$ as further discussed in Section V.

The vehicle dynamics used during the lateral maneuver are expressed as

$$\begin{aligned} \dot{x}(t) &= v(t)cos\theta(t), \quad \dot{y}(t) = v(t)sin\theta(t) \\ \dot{\theta}(t) &= v(t)tan\phi(t)/L_w, \quad \dot{\phi}(t) = \omega(t) \end{aligned} \tag{26}$$

where the physical interpretation of all variables above is shown in Fig. 4. In addition, we impose physical constraints as follows:

$$|\phi(t)| \leq \phi_{max}, \quad |\theta(t)| \leq \theta_{max} \tag{27}$$

The associated initial conditions are $\phi(t_0^L) = 0$, $\theta(t_0^L) = 0$, $y(t_0^L) = 0$. The terminal time is defined as t_f^L and the associated terminal conditions are

$$\phi(t_f^L) = 0, \quad \theta(t_f^L) = 0, \quad y(t_f^L) = l \tag{28}$$

where l is the lane width. Thus, the optimal control problem for the lateral maneuver is formulated as

$$\begin{aligned} &\min_{\phi(t), t_f^L} \int_{t_0^L}^{t_f^L} \frac{1}{2} w_\phi \phi^2(t) dt + w_{t_f^L} t_f^L \\ &\text{s.t. (26), (27), (28)} \end{aligned} \tag{29}$$

where the objective function combines both the lateral maneuver time and the associated energy approximation of the controllable vehicle. The two terms in (29) need to be properly normalized, therefore, we set $w_\phi = \frac{\rho^L}{\phi_{\max}^2}$ and $w_{t_f^L} = \frac{1-\rho^L}{T_{fmax}^L}$, where $\rho^L \in [0, 1]$ and T_{fmax}^L is set based on an empirical value as shown later in simulation results. We assume that $v(t) = v$ is constant over the lateral maneuver, which is reasonable since we will show that the lateral phase time is small compared to the longitudinal phase we have already studied.

In solving (29), there are two main challenges: (i) the problem is overconstrained due to the given initial and terminal conditions, and (ii) the high nonlinearity of the vehicle dynamics in (26) [2]. We provide next three approaches to solving the problem.

A. Numerical Solution

Problem (29) may be solved using a standard numerical solver for optimal control problems. We have used the TomLab Toolbox, a commercial solver for optimal control problems, to obtain an optimal solution. An example optimal trajectory of $\phi(t)$ is shown in Fig. 13 where it is clear that this trajectory is piecewise linear and symmetric as one might expect for such a maneuver. Thus, a generic optimal trajectory is as shown in Fig. 5. We will exploit this structure to seek an optimal solution which can be obtained in a much simpler way, hence it is also computationally much more efficient.

B. Parametric Optimization Method

Since numerical solutions reveal the structure of an optimal trajectory to be as shown in Fig. 5, we can formulate a *parametric* optimization problem where we seek to optimize the values of the parameters c, b (the slopes of the three linear segments of the trajectory) and τ_1 (the end time of the first linear segment). Therefore, the dynamics of $\phi(t)$ on an optimal trajectory are

$$\dot{\phi}(t) = \begin{cases} c & \text{if } t \leq \tau_1 \\ -b & \text{if } \tau_1 < t \leq (t_0^L + t_f^L)/2 \end{cases} \tag{30}$$

where $\tau_1 = b(t_0^L + t_f^L)/2(c+b)$ so as to ensure that $\phi(t) = 0$ when $t = (t_0^L + t_f^L)/2$. It follows that

$$\phi(t) = \begin{cases} ct & \text{if } t \le \tau_1 \\ (c+b)\tau_1 - bt & \text{if } \tau_1 < t \le (t_0^L + t_f^L)/2 \end{cases}$$

Combining this with the dynamics of $\theta(t)$ in (26), we have

$$\theta(t) = \begin{cases} -\frac{v}{cL_w}\ln(cos\phi(t)) & \text{if } t \le \tau_1 \\ -\frac{v}{cL_w}\ln(cos\phi(\tau_1)) & \\ -\frac{v}{bL_w}\ln(cos\phi(\tau_1)) & \\ +\frac{v}{bL_w}\ln(cos\phi(t)) & \text{if } \tau_1 < t \le (t_0^L + t_f^L)/2 \end{cases} \tag{31}$$

Using the expression above for $\theta(t)$ from (26), we can also derive an expression for $y(t)$ on an optimal trajectory. Unfortunately, the complexity of (31) makes it difficult to obtain an exact numerical value for $y(t)$; instead, we approximate $y(t)$ using a 10^{th} order polynomial expression where the coefficients can be expressed as functions of c, b and τ_1. Then we reformulate (29) as a parametric optimization problem in terms of c, b and τ_1 so as to obtain their optimal values c^*, b^* and τ_1^*. To compensate for the approximation error in $y(t)$, we need to adjust the parameters so as to ensure that the controllable vehicle can arrive at the terminal position when $t = t_L^f$. Based on the optimal parameters we obtain, we adjust τ_1^* to ensure that the actual terminal position is $l/2$ when $t = t_L^f$.

C. Control Barrier Function Method

Barrier functions (BFs) are Lyapunov-like functions which have recently been used in verification and control problems. Control BFs (CBFs) are extensions of BFs which, combined with control Lyapunov functions (CLFs), have been shown to allow constrained optimal control problems to be mapped onto a sequence of quadratic programs (QPs) for nonlinear systems that are affine in controls and can be solved in real time [30], [31]. We briefly review next the fundamental definitions and results which will allow us to use this approach in order to solve (29).

Definition 1 (Class $\mathcal{K}$ Function [32]): A continuous function $\kappa : [0, k) \to [0, \infty), k > 0$ is said to belong to class $\mathcal{K}$ if it is strictly increasing and $\kappa(0) = 0$.

Consider an affine control system of the form

$$\dot{\boldsymbol{s}} = f(\boldsymbol{s}) + g(\boldsymbol{s})\boldsymbol{u} \tag{32}$$

where $\boldsymbol{s} \in \mathbb{R}^n$, $f : \mathbb{R}^n \to \mathbb{R}^n$ and $g : \mathbb{R}^n \to \mathbb{R}^{n\times q}$ are locally Lipschitz, and $\boldsymbol{u} \in U \subset \mathbb{R}^q$ (U denotes the control constraint set). Solutions $\boldsymbol{s}(t)$ of (32), starting at $\boldsymbol{s}(t_0)$, $t \ge t_0$, are forward complete.

Definition 2 [33]: A set $\mathscr{C} \subset \mathbb{R}^n$ is forward invariant for system (32) if its solutions starting at all $\boldsymbol{s}(t_0) \in \mathscr{C}$ satisfy $\boldsymbol{s}(t) \in \mathscr{C}$ for $\forall t \ge t_0$.

Definition 3 [33]: Control barrier function (CBF): Let $\mathscr{C} := \{\boldsymbol{s} \in \mathbb{R}^n : h(\boldsymbol{s}) \ge 0\}$, where $h : \mathbb{R}^n \to \mathbb{R}$ is continuously differentiable. A function $B : \mathscr{C} \to \mathbb{R}$ is a control barrier function (CBF) for system (32) if there exist class $\mathcal{K}$ functions β_1, β_2 and $\gamma > 0$ such that

$$\frac{1}{\beta_1(h(\boldsymbol{s}))} \le \frac{1}{\beta_2(h(\boldsymbol{s}))}$$
$$\inf_{u\in U}[L_f B(\boldsymbol{s}) + L_g B(\boldsymbol{s})u - \frac{\gamma}{B(\boldsymbol{s})}] \le 0$$

for all $\boldsymbol{s} \in Int(\mathscr{C})$, where L_f, L_g denote the Lie derivatives along f and g, respectively, and $Int(\mathscr{C})$ is the interior of $\mathscr{C}$.

Theorem 7 [33]: Given a CBF B, any Lipschitz continuous controller $u \in K_{cbf}(\boldsymbol{s})$, with

$$K_{cbf}(\boldsymbol{s}) := \{u \in U : L_f B(\boldsymbol{s}) + L_g B(\boldsymbol{s})u - \frac{\gamma}{B(\boldsymbol{s})} \le 0\},$$

renders set $\mathscr{C}$ forward invariant for affine control system (32).

Definition 4 (Control Lyapunov Function (CLF) [31]): A continuously differentiable function $V : \mathbb{R}^n \to \mathbb{R}$ is a globally and exponentially stabilizing control Lyapunov function (CLF) for system (32) if there exist constants $c_1 > 0, c_2 > 0, c_3 > 0$ such that $c_1||\boldsymbol{s}||^2 \le V(\boldsymbol{s}) \le c_2||\boldsymbol{s}||^2$ and for $\forall \boldsymbol{s} \in \mathbb{R}^n$:

$$\inf_{u\in U}[L_f V(\boldsymbol{s}) + L_g V(\boldsymbol{s})\boldsymbol{u} + c_3 V(\boldsymbol{s})] \le 0.$$

Theorem 8 [31]: Given an exponentially stabilizing CLF V as in Def. 4, any Lipschitz continuous controller $\boldsymbol{u} \in K_{clf}(\boldsymbol{s})$, with

$$K_{clf}(\boldsymbol{s}) := \{\boldsymbol{u} \in U : L_f V(\boldsymbol{s}) + L_g V(\boldsymbol{s})\boldsymbol{u} + c_3 V(\boldsymbol{s}) \le 0\},$$

exponentially stabilizes system (32) to its zero dynamics (defined by the dynamics of the internal part if we transform the system to standard form and set the output to zero [32]).

1) Problem Formulation: We partition problem (29) into two phases. The first phase is over $[y(t_0^L), \frac{y(t_0^L)+y(t_f^L)}{2}]$ and the second is over $(\frac{y(t_0^L)+y(t_f^L)}{2}, y(t_f^L)]$. Exploiting the symmetry of the solution (see Fig. 5), we solve the problem for the first phase without the terminal condition regarding $\theta(t)$, and then mirror the optimal trajectory for the second phase as in Fig. 5. The whole symmetric trajectory of $\theta(t)$ around $t = (t_0^L + t_L^f)/2$ can guarantee that all terminal conditions in (28) can be satisfied since $\theta(t_0^L) = \theta(t_f^L) = 0$. Therefore, for the first phase, we use CBFs to map terminal constraints and limitations from states $\theta(t)$, $y(t)$ onto the controllable parameter $\phi(t)$.

Referring to Definition 3, let $\gamma = 1$ and $B_q(s(t)) = \frac{1}{h_q(s(t))}$ where $h_1(s(t)) = \phi_{max} - \phi(t)$, $h_2(s(t)) = \theta_{max} - \theta(t)$, $h_3(s(t)) = \theta(t)$ and $h_4(s(t)) = [y_f/2 - y(t)]^2 - \phi(t)$. Note that $h_4(s(t))$ is an artificial constraint which ensures that when $y(t) = y_f/2$, we have $\phi(t) = 0$. We define $V(s(t)) = (\theta(t) - \theta_{max})^2$ as the CLF so as to minimize the maneuver time since the lower bound of the maneuver time is achieved when θ_{max} is attained.

Next, we partition the time interval $[t_0^L, (t_0^L + t_L^f)/2]$ into a series of time steps $\{[t_0^L + k\Delta t, t_0^L + (k+1)\Delta t]\}, k = 0, 1, 2, \ldots$. Over each time step, we assume that the control $\phi(t)$ is constant. Applying the CBF method, over each time

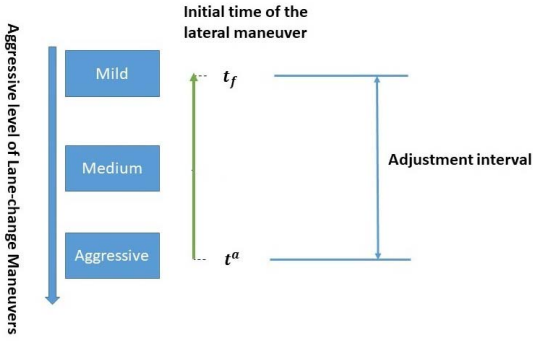

Fig. 6. Maneuver aggressiveness.

interval $[t_0^L, t_0^L + \Delta t]$ we solve the QP:

$$\begin{aligned}
&\min_{\phi(t)} \int_{t_0^L+k\Delta t}^{t_0^L+(k+1)\Delta t} \frac{1}{2}\phi^2(t)dt + p\delta^2(t) \\
&\text{s.t. } \phi(t) \geq 0, \phi(t) \leq \phi_{max}, \phi(t) \leq [y_f/2 - y(t)]^2 \\
&\underbrace{\frac{v(t)}{L_w(\theta_{max}-\theta(t))^2} tan\phi(t)}_{L_g B_2(s(t))} \leq \underbrace{(\theta_{max}-\theta(t))}_{\frac{1}{B_2(s(t))}} \\
&\underbrace{-\frac{1}{\theta^2(t)}\frac{v(t)}{L_w} tan\phi(t)}_{L_g B_3(s(t))} \leq \underbrace{\theta(t)}_{\frac{1}{B_3(s(t))}} \\
&\underbrace{2(\theta(t)-\theta_{max})\frac{v(t)}{L_w} tan\phi(t)}_{L_g V(s(t))} + \underbrace{\epsilon(\theta(t)-\theta_{max})^2}_{\epsilon V(s(t))} \leq \delta(t)
\end{aligned} \tag{33}$$

where p denotes a weight coefficient and $\delta(t)$ is a relaxation variable which we seek to minimize in a quadratic sense.

After solving a QP over each time step, we will obtain an optimal $\phi(t)$ for (33). Based on this optimal solution, we update all states and repeat the process of solving (33) over the next time step until $y(t) = y_f/2$.

V. Combination of Longitudinal and Lateral Maneuvers

After addressing the longitudinal and lateral maneuver components separately, we next consider how to integrate them into a complete lane change maneuver. The initial time t_0^L for the lateral maneuver phase is associated with a preset driver "aggressiveness" level, similar to the way we addressed the problem of minimizing the longitudinal maneuver time in (4). As illustrated in Fig. 6, the mildest (most conservative) approach is to not execute the lateral maneuver until the longitudinal phase is complete, i.e., set $t_0^L = t_f$. At the other extreme, the most aggressive approach is determined by the earliest time that any adjacent vehicle along the longitudinal direction can be guaranteed to not collide with the controllable CAV C.

Let us define the earliest times when CAV C has reached a safe distance form each of the other three CAVs involved in the longitudinal maneuver in Fig. 1:

$$\begin{aligned}
t_1^a &= \min\{t \in [t_0, t_f] : x_1(t) - x_C(t) \geq L_v\} \\
t_2^a &= \min\{t \in [t_0, t_f] : x_C(t) - x_2(t) \geq L_v\} \\
t_U^a &= \min\{t \in [t_0, t_f] : x_U(t) - x_C(t) \geq L_v\}
\end{aligned}$$

where L_v is a safe distance constant, typically determined by the length of the controllable CAV. Depending on which of *Cases 1,2,3* in Fig. 3 applies, we then set $t_0^L = t^a$ as follows:

$$\begin{aligned}
t^a &= \max\{t_1^a, t_2^a\} \quad \text{if } \textit{Case 1} \text{ applies} \\
t^a &= \max\{t_1^a, t_2^a, t_U^a\} \quad \text{if } \textit{Case 2} \text{ or } \textit{3} \text{ applies}
\end{aligned}$$

where in *Case 1* we know that the safe distance constraint between CAVs U and C which will never be violated and, therefore, it need not be included.

The above time $t_0^L = t^a$ may not always be feasible. Since we assume $v(t)$ to be constant over the lateral maneuver, there is still a risk that vehicles may collide under an aggressive setting. In order to guarantee no collision between any vehicle, we use Algorithm 2 which makes use of the following definitions. First, let $\hat{x}_C(x_C(t_0^L), v_C(t_0^L), t)$ be the position trajectory of CAV C along the longitudinal direction over the lateral maneuver. Note that $\hat{x}_C(x_C(t_0^L), v_C(t_0^L), t)$ depends on $x_C(t_0^L), v_C(t_0^L)$ and on the optimal control solution method used in Section IV. Next, we define the following collision avoidance **(CA)** condition:

$$\begin{aligned}
\textbf{(CA)}\ \forall t \in [t_0^L, t_f^L] : x_1(t) - \hat{x}_C(x_C(t_0^L), v_C(t_0^L), t) \geq L_v \\
\hat{x}_C(x_C(t_0^L), v_C(t_0^L), t) - x_2(t) \geq L_v \\
x_U(t) - \hat{x}_C(x_C(t_0^L), v_C(t_0^L), t) \geq L_v
\end{aligned}$$

We use Algorithm 2 to check whether condition **(CA)** is satisfied in order to apply the lateral maneuver. As we increase t_0^L, the chance that **(CA)** is satisfied will also increase. Note that when $t_0^L = t_f$, the distance between any adjacent vehicle is no less than the safety distance which is large enough to ensure that no collision occurs.

Algorithm 2 Determine the Initial Time of the Lateral Maneuver

```
if t ≥ t^a then
    judge=1;
    while judge=1 do
        Calculate x̂_C at the current time;
        if (CA) is satisfied then
            judge=0; t_0^L =current time;
        else
            delay Δt
        end
    end
end
```

VI. Simulation Results

In this section, we provide simulation results illustrating the time and energy-optimal maneuver controller we have derived and compare its performance to a baseline of human-driven vehicles. In what follows, we set the minimal and maximal

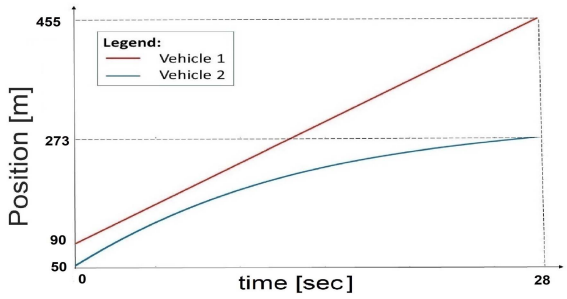

Fig. 7. Optimal Position trajectories of vehicle 1 and 2 in *Case 1* of Fig. 3.

vehicle speeds to $1m/s$ and $33m/s$ respectively and the maximal acceleration and deceleration to $3.3m/s^2$ and $-7m/s^2$ respectively. The aggressiveness coefficients α_i, $i = 1, 2$, C in (4) are set as $\alpha_1 = 0.3$, $\alpha_2 = 0.3$ and $\alpha_C = 0.2$.

A. Longitudinal Maneuver

Case 1 in Fig. 3. We set $x_1(t_0) = 90m$, $v_1(t_0) = 13m/s$, $x_U(t_0) = 100m$, $v_U(t_0) = 9m/s$, $x_2(t_0) = 50m$, $v_2(t_0) = 18m/s$ and $x_C(t_0) = 13m$, $v_C(t_0) = 10m/s$. Solving (4), we derive $t_f = 28.14s$ and after solving (5), we obtain $x_1(t_f) = 455.8m$, $x_C(t_f) = 303.24m$ and $x_2(t_f) = 273.24m$. Figures 7–8 show the optimal trajectories of all controllable vehicles. In Fig. 7, CAV 1 maintains a constant velocity which contributes a zero value to the cost in (6), while the velocity of CAV 2 decreases to create space for CAV C to change lanes. The optimal trajectory of CAV C in Fig. 8 is obtained without considering the safety constraint because of Theorem 4. CAV C keeps on accelerating and the safety distance constraint is never violated.

B. Longitudinal Maneuver

Case 2 in Fig. 3. We set $x_1(0) = 70m$, $v_1(0) = 13m/s$, $x_2(0) = 30m$, $v_2(0) = 18m/s$, $x_C(0) = 13m$, $v_C(0) = 12m/s$, $x_U(0) = 80m$, $v_U(0) = 10m/s$. Solving (4) and (5), we derive $t_f = 21.4s$ and $x_1(t_f) = 348.37m$, $x_2(t_f) = 214.13m$, $x_C(t_f) = 244.13m$. The optimal trajectories of CAVs 1,2 are similar to those of Case 1 as shown in Fig. 9 in which 1 is cruising with a constant speed and the associated surrogate energy cost defined in (3) is zero, while the velocity of CAV 2 decreases. Figure 10 shows the optimal trajectory of CAV C which, once again, is obtained without considering the safety constraint based on Theorem 5. CAV C decelerates to ensure it satisfies its terminal position while the safety constraint is never violated. We also provide a comparison between the optimal control (OC) method and the control barrier function (CBF) method [31] for all controllable vehicles in this case. As we force the terminal time under the CBF method to be the same with that of the optimal control method, the corresponding surrogate energy metric $\int_0^{t_f} u^2(t)dt$ used in (3) is 59.4 m^2/s^3, larger than that under the optimal control method, 12.6 m^2/s^3. As stated in [33], compared with the optimal control method, CBF is able to deal with nonlinear dynamic models and more complex objective functions at the expense of suboptimality.

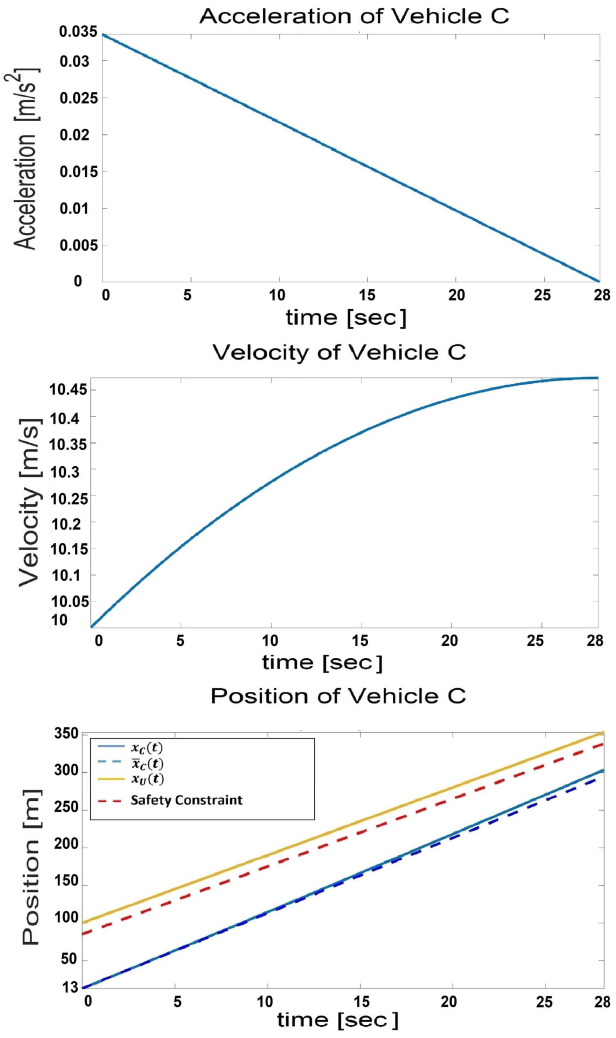

Fig. 8. Optimal trajectories of vehicle C in *Case 1* of Fig. 3.

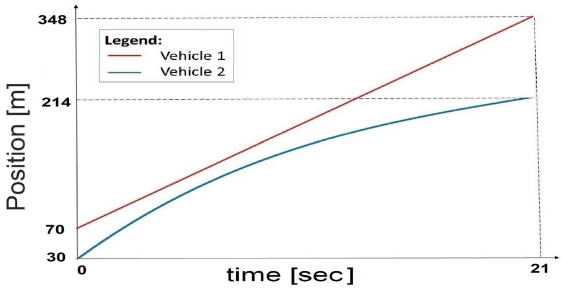

Fig. 9. Optimal Position trajectories of vehicle 1 and 2 in *Case 2* of Fig. 3.

C. Longitudinal Maneuver

Case 3 in Fig. 3. We set $x_1(0) = 40m$, $v_1(0) = 11m/s$, $x_U(0) = 40m$, $v_U(0) = 8m/s$ $x_2(0) = 10m$, $v_2(0) = 23m/s$, $x_C(0) = 13m$, $v_C(0) = 19m/s$. Solving (4) and (5), we derive $t_f = 14.49s$ and $x_1(t_f) = 199.37m$, $x_2(t_f) = 75m$, $x_C(t_f) = 105.9m$. In this case, CAV 1 accelerates and CAV 2 decelerates in order to create space for CAV C as shown in Fig. 11. For CAV C, we first solve the optimal control problem (16) without considering the safety constraint and find

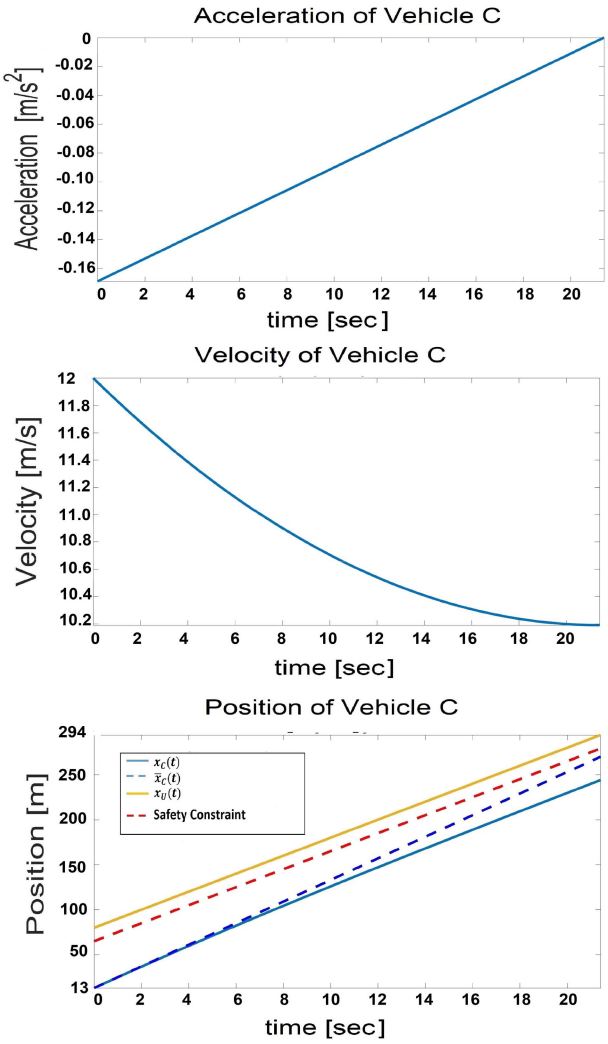

Fig. 10. Optimal trajectories of vehicle C in *Case 2* of Fig. 3.

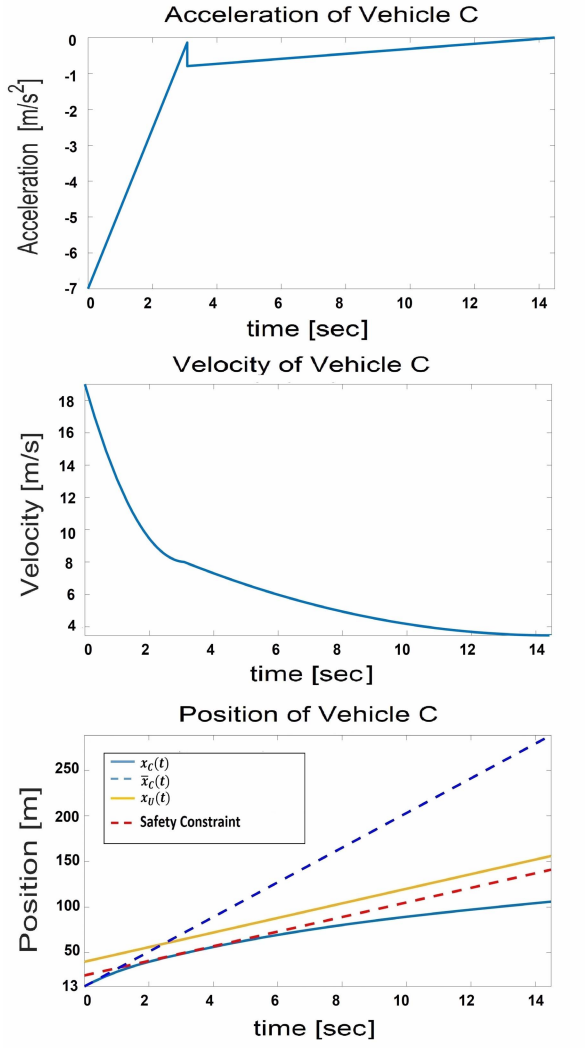

Fig. 12. Optimal trajectories of vehicle C in *Case 3* of Fig. 3.

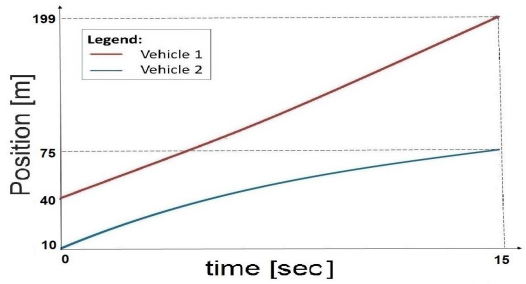

Fig. 11. Optimal Position trajectories of vehicle 1 and 2 in *Case 3* of Fig. 3.

that it actually becomes active. Therefore, we proceed with the two subproblems (19) and (20) to derive the true optimal trajectories. We obtained $a^* = 43m$ and $\tau_1^* = 3.2s$, and Fig. 12 shows the optimal trajectory of CAV C. Observe that C decelerates over the maneuver and the safety distance constraint is active at $\tau_1^* = 3.2s$ when there is a jump in the acceleration trajectory. Following that, CAV C continues decelerating until it reaches its terminal position. The computational time is around 2.3s using MATLAB R2016b on a computer with a 4-core CPU, Intel(R) Core(TM) i7-6700HQ@2.6GHz and a 16.0GB RAM.

TABLE I

COMPARISONS OF DIFFERENT VALUES OF THE AGGRESSIVENESS PARAMETERS

Aggress. Parm. / Maneuver Time [sec]	α_1	α_2	α_C
10	0.7	0.7	0.2
12	0.7	0.5	0.2
24	0.5	0.5	0.2
28	0.5	0.3	0.2

D. Longitudinal Maneuver

We include some simulation results in Table I over different values of the aggressiveness parameters under the initial conditions: $x_1(t_0) = 40m$, $v_1(t_0) = 7m/s$, $x_U(t_0) = 100m$, $v_U(t_0) = 9m/s$, $x_2(t_0) = 10m$, $v_2(t_0) = 18m/s$ and $x_C(t_0) = 13m$, $v_C(t_0) = 10m/s$. Note that aggressiveness only impacts the terminal time and terminal position of every controllable CAV without affecting the solution approach.

E. Lateral Maneuver

We set $T_{fmax}^L = 4s$, $l = 3.8m$, $L_w = 4m$, $v = 11m/s$, $\theta_{max} = 0.576$, $\phi_{max} = 0.2$, and $\rho^L = 0.5$ in (33). Solutions

TABLE II
COMPARISONS OF DIFFERENT METHODS IN LATERAL MANEUVER

Methods \ Results	Maneuver Time [sec]	Surrogate Energy defined in (29) [$\times 10^{-3}$]	Value of the Objective in (29) with $\rho^L = 0.5$
Tomlab	3.1	3.8	0.44
POM	3.0	1.6	0.40
CBF	3.5	1.2	0.45

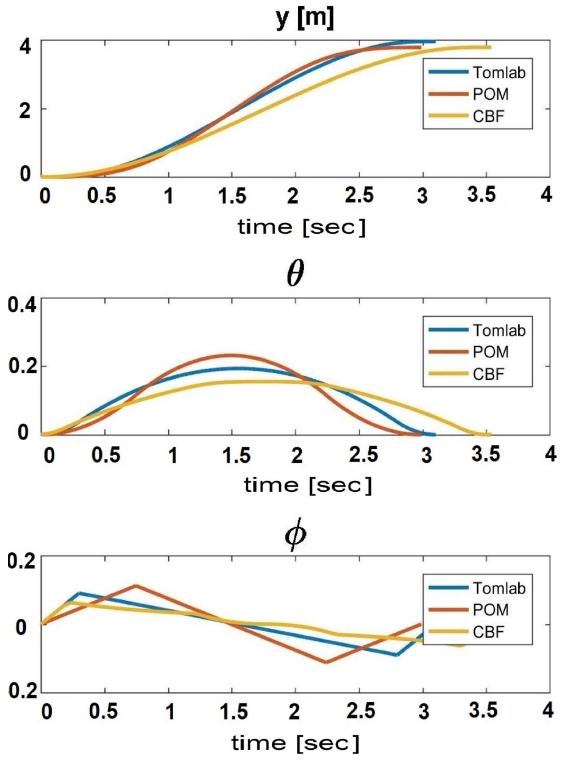

Fig. 13. Optimal Trajectories of vehicle C over the lateral maneuver.

provided by Tomlab, the parametric optimization method (POM) and CBF are compared in the following. Fig. 13 shows the trajectory of $y^*(t)$, $\theta^*(t)$ and $\phi^*(t)$ under the Tomlab. The maneuver time is $3.1s$ and associated surrogate energy consumption defined in (29) is 3.8×10^{-3}. Figures 13 also shows the trajectories of the solutions under the POM and CBF methods respectively. The associated maneuver time and surrogate energy consumption are shown in Table II. We find that the CBF achieves the least surrogate energy consumption while the POM achieves the least maneuver time. Finally, note that the lateral maneuver time is around $3s$ under all three methods. This value is relatively small compared with the longitudinal maneuver time, which makes the assumption that $v(t)$ is constant over the lateral maneuver reasonable. The computational time for POM is around 0.08s and that of the CBF method around 0.70s making them both suitable for real-time implementation. The computational time of the numerical solution using TomLab is $5s$ which is significantly larger.

TABLE III
INITIAL STATES OF VEHICLES

Cases \ States	$x_1(0)[m]$	$v_1(0)[m/s]$	$x_2(0)[m]$	$v_2(0)[m/s]$	$x_C(0)[m]$	$v_C(0)[m/s]$	$x_U(0)[m]$	$v_U(0)[m/s]$	$d_C[m]$
(1)	95	13	0	18	13	10	120	9	30
(2)	120	13	30	18	13	16	100	10	30
(3)	100	11	10	23	213	19	290	8	30

TABLE IV
ENERGY COMPARISON: CAVS VS HUMAN-DRIVEN VEHICLES

Cases \ Surrogate Energy defined in (3)	CAVs	Human-driven Vehicles	Improvement
(1)	6.8	16.4	59%
(2)	23.0	46.0	50%
(3)	59.5	103.5	43%

F. Comparison of Optimal Maneuver Control and Human-Driven Vehicles

We use standard car-following models in the commercial SUMO simulator to simulate a lane change maneuver implemented by human-driven vehicles with the requirement that vehicle C changes lanes between vehicles 1 and 2. We considered all cases in Fig. 3 with both CAVs and human-driven vehicles sharing the same initial states as shown in Table III. The associated surrogate energy consumption is shown in Table IV and provides evidence of savings in the range $43 - 59\%$ over all three cases.

VII. CONCLUSION AND FUTURE WORK

We use an optimal control framework for a Connected Automated Vehicle (CAV) cooperating with neighboring CAVs in order to implement a highway lane change maneuver consisting of a longitudinal phase and a lateral phase where it safely changes lanes. For the first phase, we optimize the maneuver time and subsequently minimize the associated surrogate energy consumption of all cooperating vehicles in this maneuver. For the second phase, we jointly optimize time and energy approximation and provide three different solution methods including a real-time approach based on Control Barrier Functions (CBFs). Our ongoing work aims to incorporate a "comfort" factor in the problem by minimizing any resulting jerk (as in Fig. 12) and adopt a more general velocity-varying safety distance constraint.

APPENDIX

Proof of Lemma 1: If $\Delta x_1^*(t_f) < 0$, then $\Delta x_1(t_f) = 0$ is a better solution since it is feasible (the distance between vehicles 1, 2 under $\Delta x_1(t_f) = 0$ is larger than under $\Delta x_1^*(t_f) < 0$) and it is obvious that it yields a lower cost in (5) than the one with $\Delta x_1^*(t_f) < 0$ (the control is $u_i(t) = 0$.) Therefore, we must have $\Delta x_1^*(t_f) \geq 0$. The proof for $\Delta x_2^*(t_f) \leq 0$ is similar. ■

Proof of Theorem 1: First, by Lemma 1, it is obvious that $u_1(t) \geq 0$ is a feasible solution of (6) since $\Delta x_1^*(t_f) \geq 0$ implies that $u_1(t) < 0$ for all $t \in [t_0, t_f]$ is not feasible. The same applies to $u_2(t) \leq 0$ being a feasible solution of (7).

Starting with vehicle 1, suppose that there exists some $[t_1, t_2) \subset [0, t_f]$ in which the optimal solution satisfies $u_1^*(t) < 0$. We will show that there exists another control which would lead to a smaller cost than $u_1^*(t)$. Consider a control $u_1^1(t)$ defined so that $u_1^1(t) = u_1^*(t) \geq 0$ for $t \in [0, t_1) \cup [t_2, t_f]$, $u_1^1(t) = 0$ for $t \in [t_1, t_2)$. It is obvious that the cost of the control $u_1^1(t)$ is lower than that of $u_1^*(t)$. $u_1^1(t)$ will not violate the safety constraint. Based on the construction of $u_1^1(t)$, it is obvious to show that $x_1^1(t) \geq x_1^*(t)$. Since we have $x_1^*(t) - x_2^*(t) \geq d_2$, we must have $x_1^1(t) - x_2^*(t) \geq d_2$. However, we have $x_1^1(t_f) > x_1^*(t_f)$ because $u_1^1(t) > u_1^*(t)$, $t \in [t_1, t_2)$, thus violating the terminal condition in (6). Therefore, we construct another control $u_1^2(t)$, a variant of $u_1^1(t)$ which is feasible, as follows. Define

$$g_1(t) = x_1^1(t) + v_1^1(t)(t_f - t) \tag{34}$$

and observe that $g_1(t)$ is a continuous function of t since $x_1^1(t)$ and $v_1^1(t)$ are continuous. Because $g_1(0) = x_1^1(0) + v_1^1(0)t_f < x_1^*(t_f)$ (by Lemma 1) and $g_1(t_f) = x_1^1(t_f) \geq x_1^*(t_f)$, there exists some $t_m \in [0, t_f]$ such that $g_1(t_m) = x_1^*(t_f)$. We now define a control $u_1^2(t)$ such that $u_1^2(t) = u_1^1(t) \geq 0$ for $t \in [0, t_m)$, $u_1^2(t) = 0$ for $t \in [t_m, t_f]$. It follows that $x_1^2(t_m) = x_1^1(t_m)$, $v_1^2(t_m) = v_1^1(t_m)$ and $x_1^2(t_f) = x_1^1(t_m) + v_1^1(t_m)(t_f - t_m)$ which implies that $x_1^2(t_f) = g_1(t_m)$ from (34). Thus, the terminal position constraint is not violated under $u_1^2(t)$. Based on the definitions of $u_1^2(t)$ and $u_1^1(t)$, it is obvious that $u_1^2(t)$ does not violate the acceleration constraints in (2). Next, we show that the velocity constraints in (2) are also not violated. Assume that for some t_n, $v_1^1(t_n) = v_{1\max}$ initiating an arc where the velocity is $v_1^1(t) = v_{1\max}$. There are two cases:

(a) If $t_n \geq t_m$, we have $v_1^1(t_m) \leq v_1^1(t_n)$ because $u_1^1(t) \geq 0$ for all $t \in [0, t_f]$. Based on the definition of $u_1^2(t)$, the maximal speed under the control $u_1^2(t)$ is $v_1^1(t_m)$ and the velocity constraint is, therefore, inactive.

(b) If $t_n < t_m$, we have $v_1^1(t_m) > v_1^1(t_n)$. Taking the time derivative of $g_1(t)$, we derive $\dot{g}_1(t) = u_1^1(t)(t_f - t) \geq 0$. It follows that

$$g_1(t_n) < g_1(t_m) = x_1^*(t_f) \tag{35}$$

where the equality follows from the definition of t_m above. Note that we do not need to consider the case that $g_1(t_n) = g_1(t_m)$ in (35) as this would lead to $\dot{g}_1(t) = 0\ \forall t \in [t_n, t_m]$, hence $u_1^1(t) = 0\ \forall t \in [t_n, t_m]$ which guarantees the velocity constraint is not violated. Then, let us construct a new control $u_1^3(t)$ such that $u_1^3(t) = u_1^*(t) \geq 0$ for $t \in [0, t_1) \cup [t_2, t_n)$, $u_1^3(t) = 0$ for $t \in [t_1, t_2) \cup [t_n, t_f]$, where $t_n \geq t_1$ because $v_1^3(t) < v_{1\max}$ for $t < t_1$ based on the feasibility of $u_1^*(t)$. Moreover, if $t_1 < t_n < t_2$, we define $u_1^3(t) = 0$ for $t > t_1$, i.e., $u_1^3(t) = u_1^*(t) \geq 0$ for $t \in [0, t_1)$, $u_1^3(t) = 0$ for $t \in [t_1, t_f]$. Based on the definition of $u_1^3(t)$, we have $u_1^3(t) = u_1^1(t)$ for $t \in [0, t_n)$. Therefore, $x_1^3(t_n) = x_1^1(t_n)$ and $v_1^3(t_n) = v_1^1(t_n)$ so that (35) holds under $u_1^3(t)$. When $t \geq t_n$, we have $u_1^3(t) = 0$, therefore, $x_1^3(t_f) = x_1^1(t_n) + v_1^1(t_n)(t_f - t_n) = g_1(t_n)$ from (34). Since $v_1^3(t) = v_{1\max}$ for $t \in [t_n, t_f]$ and $x_1^3(t) \geq x_1^*(t)$ for $t \in [0, t_n)$, it is clear that $x_1^3(t_f) \geq x_1^*(t_f)$. However, since $g_1(t_n) = x_1^3(t_f) \geq x_1^*(t_f)$, this contradicts (35). We conclude that $t_n < t_m$ is not possible. Furthermore, it is also simple to show that $x_1^2(t) \geq x_1^*(t)$ based on the definition of $u_1^2(t)$, so the safety constraint will not be violated under this auxiliary control policy.

In summary, we have shown that the velocity constraint is inactive for control $u_1^2(t)$. Therefore, $u_1^2(t)$ is feasible and results in a lower cost in (6) than $u_1^*(t)$ since it includes a trajectory arc over which $u_1^2(t) = 0$. This contradicts the optimality of $u_1^*(t)$ and we conclude that the optimal control cannot contain any interval over which $u_1^*(t) < 0$.

Next, consider vehicle 2 and suppose that there exists some $[t_1, t_2) \subset [0, t_f]$ in which the optimal solution satisfies $u_2^*(t) > 0$. Consider a control $u_2^1(t)$ defined so that $u_2^1(t) = u_2^*(t) \leq 0$ for $t \in [0, t_1) \cup [t_2, t_f]$, $u_1^1(t) = 0$ for $t \in [t_1, t_2)$. It is clear that the cost under $u_2^1(t)$ is lower than that of $u_2^*(t)$ and that the acceleration constraint in (2) is inactive for $u_2^1(t)$. Furthermore, it is obvious that $x_2^*(t) \geq x_2^1(t)$ and $v_2^*(t) \geq v_2^1(t)$ for $t \in [0, t_f]$. Therefore, the terminal position inequality in (7) is not violated. Based on the definition of the safety distance constraint, $d_2(v_2(t)) = \phi v_2(t) + \delta$ is monotonically increasing in $v_2(t)$. Therefore, we conclude that the safety constraint under $u_2^1(t)$ will not be violated, since $u_2^*(t)$ is feasible and $x_2^*(t) \geq x_2^1(t)$, $v_2^*(t) \geq v_2^1(t)$. Finally, we consider the speed constraint in (2) which may be active under $u_2^1(t)$. There are two cases:

(a) If $v_2^1(t_f) > v_{2\min}$, the speed constraint is inactive under $u_2^1(t)$ over all $t \in [0, t_f]$ and $u_2^1(t)$ is a feasible solution which results in a lower cost in (7) than $u_2^*(t)$ since it includes a trajectory arc over which $u_2^2(t) = 0$.

(b) If $v_2^1(t_f) \leq v_{2\min}$, there must exist some $t_n \in [t_1, t_f]$ such that $v_2^1(t_m) = v_{2\min}$. Let us construct a new control $u_2^2(t)$ as follows: $u_2^2(t) = u_2^1(t) \leq 0$ for $t \in [0, t_m)$, $u_2^2(t) = 0$ for $t \in [t_m, t_f]$. For $t \in [0, t_m)$, it is obvious that $x_2^*(t) \geq x_2^2(t)$ and $v_2^*(t) \geq v_2^2(t)$ based on the definition of $u_2^1(t)$. For $t \in [t_m, t_f]$, vehicle 2 moves at the minimal speed $v_{2\min}$ under $u_2^2(t)$, therefore, $x_2^*(t_f) \geq x_2^2(t_f)$, that is, the terminal position inequality is satisfied. Also, it is obvious that the acceleration and the speed constraints are not violated over $[0, t_f]$. Finally, we have shown that $u_2^1(t)$ does not violate the safety constraint. Based on the same argument, it is straightforward to show that $u_2^2(t)$ will not violate this constraint, since $x_2^2(t) \leq x_2^*(t)$ and $v_2^2(t) \leq v_2^*(t)$. Therefore, $u_2^2(t)$ is feasible in (7) and the corresponding cost is lower than that of $u_2^*(t)$ because the trajectory segment with $u_2^2(t) = 0$ contributes to zero cost. We conclude that the optimal control $u_2^*(t)$ cannot contain any time interval with $u_2^*(t) > 0$. ■

Proof of Theorem 2: Problem (6) is of the same form as the fixed terminal time optimal control Problem 3 in [28] whose solution when $u_1^*(t) \geq 0$ is given in Theorem 2 of [28] and is therefore omitted. By Pontryagin's principle applied to (9), $u_1^*(t) = \min\{u_{1\max}, -\lambda_v(t)\}$ and the key parts of the proof in [28] are showing that $\eta_3(t) = 0$ and that $\lambda_v(t)$ is continuous for all $t \in [0, t_f]$. ■

Proof of Theorem 3: Problem (7) is also of the same form as the fixed terminal time optimal control Problem 3 in [28] whose solution when $u_2^*(t) \leq 0$ is given in Theorem 3 of [28] and is therefore omitted. ■

Proof of Lemma 2: Assume that at time t_k, we have $x_U(0) + v_U(0)t_k - x_C(t_k) = d_C$ and define $f(t) = x_U(0) +$

$v_U(0)t - x_C(t)$. Using a contradiction argument, if $v_C(t) \neq v_U(0)$ there are two cases: (i) If $v_C(t_k) > v_U(0)$, since $f'(t_k) = v_U(0) - v_C(t_k) < 0$, we have $f(t_k^-) > f(t_k)$, which implies $x_U(0) + v_U(0)t_k^- - x_C(t_k^-) > d_C$, therefore, the safety constraint is violated at t_k^-. (ii) If $v_C(t_k) < v_U(0)$, since $f'(t_k) = v_U(0) - v_C(t_k) > 0$, we have $f(t_k^+) > f(t_k)$, which implies $x_U(0) + v_U(0)t_k^+ - x_C(t_k^+) > d_C$, therefore, the safety constraint is violated at t_k^+. We conclude that $v_C(t_k) = v_U$ which completes the proof. ■

Proof of Theorem 4: Case 1 involves a non-strict inequality regarding the order of $\bar{x}_C(t_f)$ and $x_C(t_f)$. We first consider the strict inequality, that is, $\bar{x}_C(t_f) < x_C(t_f) \leq x_U(t_f) - d_C$. The condition $x_C(t_f) > \bar{x}_C(t_f)$ implies that $u_C(t) \geq 0$ is a feasible solution of (16) since $u_C(t) < 0$ for all $t \in [t_0, t_f]$ cannot satisfy this condition. Suppose that there exists some $[t_1, t_2) \subset [0, t_f]$ in which the optimal solution satisfies $u_C^*(t) < 0$. We will show that there exists another control which would lead to a lower cost than $u_C^*(t)$. First, we construct a control $u_C^1(t)$ such that $u_C^1(t) = u_C^*(t) \geq 0$ for $t \in [0, t_1) \cup [t_2, t_f]$, $u_C^1(t) = 0$ for $t \in [t_1, t_2)$. It is clear that $u_C^1(t)$ will not violate the acceleration constraint (2). However, the terminal position constraint is violated. Therefore, we will construct $u_C^2(t)$, a variant of $u_C^1(t)$ as follows, and will show that $u_C^2(t)$ is feasible.

First, define

$$g_C(t) = x_C^1(t) + v_C^1(t)(t_f - t) \tag{36}$$

and note that $g_C(t)$ is continuous in t since $x_C^1(t)$ and $v_C^1(t)$ are continuous. Because $g_C(0) = \bar{x}_C(t_f) < x_C^*(t_f)$ by assumption and $g_C(t_f) = x_C^1(t_f) \geq x_C^*(t_f)$, there exists some $t_m \in [0, t_f]$ such that $g_C(t_m) = x_C^*(t_f)$. We can now construct $u_C^2(t)$ such that $u_C^2(t) = u_C^1(t) \geq 0$ for $t \in [0, t_m)$, $u_C^2(t) = 0$ for $t \in [t_m, t_f]$. Observe that $x_C^2(t_f) = g_C(t_m) = x_C^*(t_f)$. Moreover, based on its definition, it is obvious that it will not violate the acceleration constraint. Next, we show that the velocity constraint is also not violated. Suppose there exists some time t_n such that $v_C^1(t_n) = v_{C\max}$ so that the trajectory may include an arc over which $v_C^1(t) = v_{C\max}$. There are two cases:

(a) If $t_n \geq t_m$, we have $v_C^1(t_m) \leq v_C^1(t_n)$ because $u_C^1(t) \geq 0$. Based on the definition of $u_C^1(t)$, the maximal speed is $v_C^1(t_m)$ and the velocity constraint is not violated.

(b) If $t_n < t_m$, we have $v_C^1(t_m) > v_C^1(t_n)$. Taking the time derivative of $g_C(t)$, we derive $\dot{g}_C(t) = u_C^1(t)(t_f - t) \geq 0$. Therefore,

$$g_C(t_n) < g_C(t_m) = x_C^*(t_f) \tag{37}$$

Note that we do need to consider the case that $g_C(t_n) = g_C(t_m)$ in (37) as this would lead to $\dot{g}_C(t) = 0\ \forall t \in [t_n, t_m]$, hence $u_C^1(t) = 0\ \forall t \in [t_n, t_m]$ which guarantees the velocity constraint is not violated. We then construct a control $u_C^3(t)$ such that $u_C^3(t) = u_C^*(t) \geq 0$ for $t \in [0, t_1) \cup [t_2, t_n]$, $u_C^3(t) = 0$ for $t \in [t_1, t_2) \cup [t_n, t_f]$. Note that $t_n \geq t_1$ because $v_C^*(t) \neq v_{C\max}$ when $t < t_1$ based on the definition of $u_C^*(t)$. If $t_1 < t_n < t_2$, we define $u_C^3(t) = 0$ when $t > t_1$ as follows: $u_C^3(t) = u_C^*(t) \geq 0$, for $t \in [0, t_1)$, $u_C^3(t) = 0$, for $t \in [t_1, t_f]$. From the construction of $u_C^3(t)$, we have $x_C^3(t_n) = x_C^1(t_n)$, $v_C^3(t_n) = v_C^1(t_n)$ so that (37) holds under $u_1^3(t)$, and $x_C^3(t_f) = g_C(t_n)$. Because $v_C^3(t) = v_{C\max}$ for $t \in [t_n, t_f]$ and $u_C^3(t) \geq u_C^*(t)$ for $t \in [0, t_n)$, it is clear that $x_C^3(t) \geq x_C^*(t)$ for all $t \in [0, t_f]$. However, this contradicts (37) since $x_C^3(t_f) = g_C(t_n) < x_C^*(t_f)$. We conclude that $t_n < t_m$ is not possible.

In summary, we have proved that the speed constraint will not be violated under the control $u_C^2(t)$. Next, we show that $u_C^2(t)$ will also not violate the safety constraint. Suppose that at time $t_\sigma \in [0, t_f)$, the safety constraint is active under control $u_C^2(t)$, i.e., $x_C^2(t_\sigma) = x_U(t_\sigma) - d_C$. Because the safety constraint is inactive at $t = t_\sigma^-$, that is, $x_C^2(t_\sigma^-) < x_U(t_\sigma^-) - d_C$, we must have $v_C^2(t_\sigma^-) > v_U(t_\sigma^-)$ to activate the constraint. Because $u_C^2(t) \geq 0$, we have $v_C^2(t_\sigma) > v_U(t_\sigma)$ which contradicts Lemma 2 leading to $x_C^2(t_\sigma^+) > x_U(t_\sigma^+) - d_C$. Since $u_C^2(t) \geq 0$, we eventually have $x_C^2(t_f) > x_U(t_f) - d_C$ which contradicts $x_C^2(t_f) = x_C^*(t_f) \leq x_U(t_f) - d_C$. Therefore, the safety constraint will not be activated over $(0, t_f)$.

We conclude that $u_C^2(t)$ is a feasible solution. Moreover, under $u_C^2(t)$ the cost is lower than that of $u_C^*(t)$ because $u_C^2(t)$ contains a segment with $u_C^2(t) = 0$ that contributes zero cost in (16) relative to $u_C^*(t)$. Therefore, the optimal control $u_C^*(t)$ cannot contain any time interval with $u_C^*(t) < 0$.

Next, we use a similar argument as above to show that the safety constraint will be inactive under the optimal control $u_C^*(t)$, that is, $\eta_5^*(t) = 0$. Assume that at time $t_\eta \in (0, t_f)$, $\eta_5^*(t_\eta) > 0$. Because the safety constraint is active at t_η and is not violated at t_f, vehicle C must have decelerated to relax the safety constraint. However, this violates the fact that $u_C^*(t) \geq 0$ as shown above. Therefore, we conclude that $\eta_5^*(t) = 0$ for all $t \in [0, t_f)$. This completes the proof for the inequalities situation.

Finally, if the equality case $\bar{x}_C(t_f) = x_C(t_f)$ applies, it is easy to see that we have $u_C^*(t) = 0\ \forall t \in (t_0, t_f)$. This completes the proof. ■

Proof of Theorem 6: The proof is similar to Theorem 4. The only difference is in the way we prove that the constructed control $u_C^2(t)$ will not violate the safety constraint. Suppose that there exists some $[t_1, t_2) \subset [0, t_f]$ in which the optimal solution satisfies $u_C^*(t) > 0$. First, we construct a control $u_C^1(t)$ such that $u_C^1(t) = u_C^*(t) \leq 0$ for $t \in [0, t_1) \cup [t_2, t_f]$, $u_C^1(t) = 0$ for $t \in [t_1, t_2)$. It is clear that $x_C^*(t) \geq x_C^1(t)$, $v_C^*(t) \geq v_C^1(t)$, $t \in [0, t_f]$. Considering the safety constraint in (16), note that if $u_C^*(t)$ does not violate the safety constraint, then neither does $u_C^1(t)$.

Using $g_C(t)$ defined in (36), note that $g_C(0) = x_C^1(0) + v_C^1(0)t_f = \bar{x}_C(t_f)$ and $g_C(t_f) = x_C^1(t_f)$. Since $x_C^1(t_f) \leq x_C^*(t_f) \leq \bar{x}_C(t_f)$ and $g_C(t)$ is continuous, there exists $t_m \in (0, t_f)$ such that $g_C(t_m) = x_C^*(t_f)$. Then, we construct $u_C^2(t) = u^1(t) \leq 0$ for $t \in [0, t_m)$ and $u_C^2(t) = 0$ for $[t_m, t_f]$. Similar to the proof of Theorem 4, $x_C^2(t_f) = g_C(t_m) = x_C^*(t_f)$. Since $u_C^2(t) = u_C^1(t)$ for $t \in [0, t_m)$, control $u_C^2(t)$ will not violate the safety constraint when $t \leq t_m$. For $t > t_m$, we have $u_C^2(t) = 0$ and $x_C^2(t)$ is linear in t with $v_C^1(t_m) > 0$. Moreover, $x_C^1(t_m) \leq x_U(t_m) - d_C$ and $x_C^2(t_f) = x_C^*(t_f) \leq x_U(t_f) - d_C$. We conclude that $u_C^2(t)$, $t \in [t_m, t_f]$, will not violate the safety constraint because the upper bound of vehicle C's safe position, $x_U(t) - d_C$, is also linear in t. Based on the definition of $u_C^2(t)$, it is obvious that it will not violate the acceleration constraint. We can then use the same argument as in the proof

of Theorem 4 to show that $v_C(t_m) \geq v_{C\min}$. Therefore, $u_C^2(t)$ is a feasible solution. It is also obvious that the cost of $u_C^2(t)$ is lower than that of $u_C^*(t)$ because $u_C^2(t)$ contains a segment with $u_C^2(t) = 0$. Therefore, the optimal control $u_C^*(t)$ cannot contain any time interval with $u_C^*(t) > 0$. This completes the proof. ■

REFERENCES

[1] S. Lam and J. Katupitiya, "Cooperative autonomous platoon maneuvers on highways," in *Proc. IEEE/ASME Int. Conf. Adv. Intell. Mechatronics*, Jul. 2013, pp. 1152–1157.

[2] B. Li, Y. Zhang, Y. Ge, Z. Shao, and P. Li, "Optimal control-based online motion planning for cooperative lane changes of connected and automated vehicles," in *Proc. IEEE/RSJ Int. Conf. Intell. Robots Syst. (IROS)*, Sep. 2017, pp. 3689–3694.

[3] P. Varaiya, "Smart cars on smart roads: Problems of control," *IEEE Trans. Autom. Control*, vol. 38, no. 2, pp. 195–207, 1993.

[4] D. Zhao, X. Huang, H. Peng, H. Lam, and D. J. LeBlanc, "Accelerated evaluation of automated vehicles in car-following maneuvers," *IEEE Trans. Intell. Transp. Syst.*, vol. 19, no. 3, pp. 733–744, Mar. 2018.

[5] M. Wang, W. Daamen, S. P. Hoogendoorn, and B. van Arem, "Cooperative car-following control: Distributed algorithm and impact on moving jam features," *IEEE Trans. Intell. Transp. Syst.*, vol. 17, no. 5, pp. 1459–1471, May 2016.

[6] M. Wang, S. P. Hoogendoorn, W. Daamen, B. van Arem, and R. Happee, "Game theoretic approach for predictive lane-changing and car-following control," *Transp. Res. C, Emerg. Technol.*, vol. 58, pp. 73–92, Sep. 2015.

[7] J. L. Fleck, C. G. Cassandras, and Y. Geng, "Adaptive quasi-dynamic traffic light control," *IEEE Trans. Control Syst. Technol.*, vol. 24, no. 3, pp. 830–842, May 2016.

[8] K. Dresner and P. Stone, "A multiagent approach to autonomous intersection management," *J. Artif. Intell. Res.*, vol. 31, pp. 591–656, Mar. 2008.

[9] A. A. Malikopoulos, C. G. Cassandras, and Y. J. Zhang, "A decentralized energy-optimal control framework for connected automated vehicles at signal-free intersections," *Automatica*, vol. 93, pp. 244–256, Jul. 2018.

[10] J. Nilsson, M. Brannstrom, E. Coelingh, and J. Fredriksson, "Longitudinal and lateral control for automated lane change maneuvers," in *Proc. Amer. Control Conf. (ACC)*, Jul. 2015, pp. 1399–1404.

[11] C. Bax, P. Leroy, and M. P. Hagenzieker, "Road safety knowledge and policy: A historical institutional analysis of The Netherlands," *Transp. Res. F, Traffic Psychol. Behav.*, vol. 25, pp. 127–136, Jul. 2014.

[12] F. You, R. Zhang, G. Lie, H. Wang, H. Wen, and J. Xu, "Trajectory planning and tracking control for autonomous lane change maneuver based on the cooperative vehicle infrastructure system," *Expert Syst. Appl.*, vol. 42, no. 14, pp. 5932–5946, Aug. 2015.

[13] M. Werling, J. Ziegler, S. Kammel, and S. Thrun, "Optimal trajectory generation for dynamic street scenarios in a Frenét frame," in *Proc. IEEE Int. Conf. Robot. Autom.*, May 2010, pp. 987–993.

[14] D. Bevly *et al.*, "Lane change and merge maneuvers for connected and automated vehicles: A survey," *IEEE Trans. Intell. Vehicles*, vol. 1, no. 1, pp. 105–120, Mar. 2016.

[15] J. Nilsson, M. Brannstrom, E. Coelingh, and J. Fredriksson, "Lane change maneuvers for automated vehicles," *IEEE Trans. Intell. Transp. Syst.*, vol. 18, no. 5, pp. 1087–1096, May 2017.

[16] Y. Luo, Y. Xiang, K. Cao, and K. Li, "A dynamic automated lane change maneuver based on vehicle-to-vehicle communication," *Transp. Res. C, Emerg. Technol.*, vol. 62, pp. 87–102, Jan. 2016.

[17] H. N. Mahjoub, A. Tahmasbi-Sarvestani, H. Kazemi, and Y. P. Fallah, "A learning-based framework for two-dimensional vehicle maneuver prediction over V2 V networks," in *Proc. IEEE 15th Intl Conf Depend., Autonomic Secure Comput., 15th Int. Conf. Pervas. Intell. Comput., 3rd Int. Conf. Big Data Intell. Comput. Cyber Sci. Technol. Congr. (DASC/PiCom/DataCom/CyberSciTech)*, Nov. 2017, pp. 156–163.

[18] H. Kazemi, H. N. Mahjoub, A. Tahmasbi-Sarvestani, and Y. P. Fallah, "A learning-based stochastic MPC design for cooperative adaptive cruise control to handle interfering vehicles," *IEEE Trans. Intell. Vehicles*, vol. 3, no. 3, pp. 266–275, Sep. 2018.

[19] Q. Wang, B. Ayalew, and T. Weiskircher, "Predictive maneuver planning for an autonomous vehicle in public highway traffic," *IEEE Trans. Intell. Transp. Syst.*, vol. 20, no. 4, pp. 1303–1315, Apr. 2019.

[20] Z. Huang, D. Chu, C. Wu, and Y. He, "Path planning and cooperative control for automated vehicle platoon using hybrid automata," *IEEE Trans. Intell. Transp. Syst.*, vol. 20, no. 3, pp. 959–974, Mar. 2019.

[21] Y. Zheng, B. Ran, X. Qu, J. Zhang, and Y. Lin, "Cooperative lane changing strategies to improve traffic operation and safety nearby freeway off-ramps in a connected and automated vehicles environment," *IEEE Trans. Intell. Transp. Syst.*, vol. 21, no. 11, pp. 4605–4614, Nov. 2020.

[22] M. A. S. Kamal, M. Mukai, J. Murata, and T. Kawabe, "Model predictive control of vehicles on urban roads for improved fuel economy," *IEEE Trans. Control Syst. Technol.*, vol. 21, no. 3, pp. 831–841, May 2013.

[23] A. Katriniok, J. P. Maschuw, F. Christen, L. Eckstein, and D. Abel, "Optimal vehicle dynamics control for combined longitudinal and lateral autonomous vehicle guidance," in *Proc. Eur. Control Conf. (ECC)*, Jul. 2013, pp. 974–979.

[24] R. Chen, C. G. Cassandras, and A. Tahmasbi-Sarvestani, "Time and energy-optimal lane change maneuvers for cooperating connected and automated vehicles," in *Proc. IEEE 58th Conf. Decis. Control (CDC)*, Dec. 2019, pp. 2220–2225.

[25] K. Vogel, "A comparison of headway and time to collision as safety indicators," *Accident Anal. Prevention*, vol. 35, no. 3, pp. 427–433, May 2003.

[26] Y. Zhang, C. G. Cassandras, and A. A. Malikopoulos, "Optimal control of connected automated vehicles at urban traffic intersections: A feasibility enforcement analysis," in *Proc. Amer. Control Conf. (ACC)*, May 2017, pp. 3548–3553.

[27] J. Rios-Torres, A. Malikopoulos, and P. Pisu, "Online optimal control of connected vehicles for efficient traffic flow at merging roads," in *Proc. IEEE 18th Int. Conf. Intell. Transp. Syst.*, Sep. 2015, pp. 2432–2437.

[28] X. Meng and C. G. Cassandras, "Optimal control of autonomous vehicles for non-stop signalized intersection crossing," in *Proc. IEEE Conf. Decis. Control (CDC)*, Dec. 2018, pp. 6988–6993.

[29] A. E. Bryson, *Applied Optimal Control: Optimization Estimation and Control*. London, U.K.: Routledge, 2018.

[30] W. Xiao, C. G. Cassandras, and C. Belta, "Decentralized merging control in traffic networks with noisy vehicle dynamics: A joint optimal control and barrier function approach," in *Proc. IEEE Intell. Transp. Syst. Conf. (ITSC)*, Oct. 2019, pp. 3162–3167.

[31] A. D. Ames, K. Galloway, and J. W. Grizzle, "Control Lyapunov functions and hybrid zero dynamics," in *Proc. IEEE 51st IEEE Conf. Decis. Control (CDC)*, Dec. 2012, pp. 6837–6842.

[32] H. K. Khalil, *Nonlinear System*, 3rd ed. Upper Saddle River, NJ, USA: Prentice-Hall, 2002.

[33] W. Xiao, C. Belta, and C. G. Cassandras, "Decentralized merging control in traffic networks: A control barrier function approach," *Proc. 10th ACM/IEEE Int. Conf. Cyber-Phys. Syst.*, 2019, pp. 270–279.

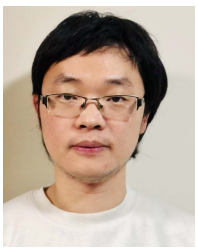

Rui Chen received the B.S. degree from the School of Automation, Huazhong University of Science and Technology, Wuhan, China, in 2011, and the M.S. degree from the School of Electronic Information and Electrical Engineering, Shanghai Jiao Tong University, Shanghai, China, in 2014. He is currently pursuing the Ph.D. degree in systems engineering with Boston University, Boston, MA, USA. His research interests include traffic light control problems, the optimization of ride sharing systems, and the optimal control of connected and autonomous vehicles.

Christos G. Cassandras (Life Fellow, IEEE) received the B.S. degree from Yale University, New Haven, CT, USA, in 1977, the M.S.E.E. degree from Stanford University, Stanford, CA, USA, in 1978, and the M.S. and Ph.D. degrees from Harvard University, Cambridge, MA, USA, in 1979 and 1982, respectively. He was with ITP Boston, Inc., Cambridge, from 1982 to 1984, where he was involved in the design of automated manufacturing systems. From 1984 to 1996, he was a Faculty Member with the Department of Electrical and Computer Engineering, University of Massachusetts Amherst, Amherst, MA, USA. He is currently a Distinguished Professor of engineering with Boston University, Boston, MA, USA, the Head of the Division of Systems Engineering, and a Professor of electrical and computer engineering. He specializes in the areas of discrete event and hybrid systems, cooperative control, stochastic optimization, and computer simulation, with applications to computer and sensor networks, manufacturing systems, and transportation systems. He has authored over 450 refereed articles in these areas, and six books. He is also a member of Phi Beta Kappa and Tau Beta Pi. He is also a fellow of the International Federation of Automatic Control (IFAC). He was a recipient of several awards, including the 2011 IEEE Control Systems Technology Award, the 2006 Distinguished Member Award of the IEEE Control Systems Society, the 1999 Harold Chestnut Prize (IFAC Best Control Engineering Textbook), a 2011 prize and a 2014 prize for the IBM/IEEE Smarter Planet Challenge competition, the 2014 Engineering Distinguished Scholar Award at Boston University, several honorary professorships, a 1991 Lilly Fellowship, and a 2012 Kern Fellowship. He was the Editor-in-Chief of the IEEE TRANSACTIONS ON AUTOMATIC CONTROL from 1998 to 2009. He serves on several editorial boards and has been a Guest Editor for various journals. He was the President of the IEEE Control Systems Society in 2012.

Amin Tahmasbi-Sarvestani received the M.S. degree in artificial intelligence from the Sharif University of Technology, Tehran, Iran, in 2011, and the Ph.D. degree from West Virginia University, Morgantown, WV, USA, in 2016. From 2016 to 2019, he was a Researcher with Honda Research and Development Americas (HRA), Inc., Ann Arbor, MI, USA. His current research interests include perception and planning for autonomous driving, machine learning, control systems, and intelligent transportation systems.

Shigenobu Saigusa received the M.Sc.Eng. degree from the University of Tsukuba, Japan, in 2000. He is currently a Chief Engineer with Honda Research and Development Americas (HRA), Inc., Ann Arbor, MI, USA. He has more than 15years of work experience in ADAS domain. He is also leading connected and automated vehicle (CAV) related ideation and technology exploration activity in HRA.

Hossein Nourkhiz Mahjoub (Member, IEEE) received the B.Sc. and M.Sc. degrees from the University of Tehran, Tehran, Iran, in 2008 and 2003, respectively, all in electrical engineering (systems communications), and the Ph.D. degree from the University of Central Florida, Orlando, FL, USA, in 2019. He has been a Ph.D. Researcher with Honda Research and Development Americas (HRA), Inc., Ann Arbor, MI, USA, since 2019. He has more than nine years of work experience in the telecommunications industry before starting his Ph.D. in 2015. His research interests include vehicle-to-everything (V2X) communications technologies, wireless channel modeling, stochastic systems analysis, and vehicular ad-hoc networks.

Yasir Khudhair Al-Nadawi received the B.Sc. and M.Sc. degrees in control and systems engineering from the University of Technology, Baghdad, Iraq, in 2008 and 2005, respectively. He is currently pursuing the Ph.D. degree with Michigan State University, East Lansing, MI, USA. He is also an Automated Vehicle Controls Research Engineer with Honda Research and Development Americas, Inc., Ann Arbor, MI, USA. His research interests include nonlinear control systems design and analysis, in particular multi-time-scales approaches, singular perturbation theory, sliding mode control theory, disturbance observers, and regulation theory.